SSD-TR-91-22

AEROSPACE REPORT NO.
TR-0091(6508-21)-1

Space Shuttle Overhead Windows, Optical Tests, Final Report

Prepared by

K. P. SCOTT
Optical Systems Department
Electronics and Sensors Division
Engineering Group

June 1991

Prepared for

SPACE SYSTEMS DIVISION
AIR FORCE SYSTEMS COMMAND
Los Angeles Air Force Base
P. O. Box 92960
Los Angeles, CA 90009-2960

Contract No. F04701-88-C-0089

Programs Group

THE AEROSPACE CORPORATION
El Segundo, California

This final report was submitted by The Aerospace Corporation, El Segundo, CA 90245-4691, under Contract No. F04701-88-C-0089 with the Space Systems Division, P.O. Box 92960, Los Angeles, CA 90009-2960. It was reviewed and approved for The Aerospace Corporation by J. Breedlove, Principal Director, Sensor Systems Subdivision, Electronics and Sensors Division, Engineering and Technology Group and H. E. Wang, Principal Director, Space Test, Space Launch Operations, Programs Group. The project officer was Capt. Ralph G. Hull III, SSD/CLPD.

This report has been reviewed by the Public Affairs Office (PAS) and is releasable to the National Technical Information Service (NTIS). At NTIS, it will be available to the general public, including foreign nationals.

This technical report has been reviewed and is approved for publication. Publication of this report does not constitute Air Force approval of the report's findings or conclusions. It is published only for the exchange and stimulation of ideas.

Ralph G. Hull, Capt, USAF

DISCLAIMER NOTICE

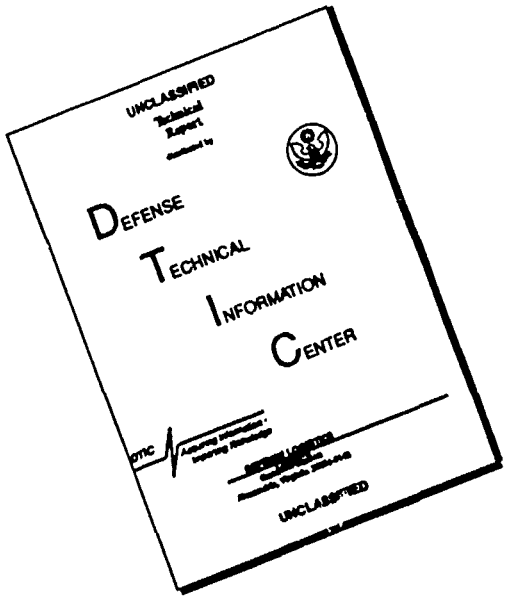

THIS DOCUMENT IS BEST QUALITY AVAILABLE. THE COPY FURNISHED TO DTIC CONTAINED A SIGNIFICANT NUMBER OF PAGES WHICH DO NOT REPRODUCE LEGIBLY.

REPORT DOCUMENTATION PAGE

1a REPORT SECURITY CLASSIFICATION Unclassified	1b RESTRICTIVE MARKINGS
2a SECURITY CLASSIFICATION AUTHORITY	3 DISTRIBUTION/AVAILABILITY OF REPORT Approved for public release; distribution unlimited
2b DECLASSIFICATION/DOWNGRADING SCHEDULE	
4 PERFORMING ORGANIZATION REPORT NUMBER(S) TR-0091(6508-21)-1	5 MONITORING ORGANIZATION REPORT NUMBER(S) SSD-TR-91-22
6a NAME OF PERFORMING ORGANIZATION The Aerospace Corporation 6b. OFFICE SYMBOL *(If applicable)*	7a NAME OF MONITORING ORGANIZATION Space Systems Division Air Force Systems Command
6c ADDRESS *(City, State, and ZIP Code)* 2350 E. El Segundo Blvd. El Segundo, CA 90245-4691	7b. ADDRESS *(City, State, and ZIP Code)* Los Angeles Air Force Base P. O. Box 92960 Los Angeles, CA 90009-2960
8a NAME OF FUNDING/SPONSORING ORGANIZATION Space Systems Division Air Force Systems Command 8b OFFICE SYMBOL *(If applicable)*	9. PROCUREMENT INSTRUMENT IDENTIFICATION NUMBER
8c ADDRESS *(City, State, and ZIP Code)*	10. SOURCE OF FUNDING NUMBERS PROGRAM ELEMENT NO / PROJECT NO. / TASK NO / WORK UNIT ACCESSION NO

11 TITLE *(Include Security Classification)*
Space Shuttle Overhead Window Optical Tests, Final Report

12 PERSONAL AUTHOR(S)
Karen P. Scott

13a TYPE OF REPORT	13b TIME COVERED	14. DATE OF REPORT *(Year, Month, Day)*	15. PAGE COUNT
TR	FROM 8-1-89 TO 8-3-89	June 1991	82

16. SUPPLEMENTARY NOTATION

17 COSATI CODES			18 SUBJECT TERMS *(Continue on reverse if necessary and identify by block number)*
FIELD	GROUP	SUB-GROUP	Window(s), Spacecraft, Space Shuttle Window, Optics, Resolution, Space Shutte

19 ABSTRACT *(Continue on reverse if necessary and identify by block number)*

Visual photographic, and interferometric tests were performed on the space shuttle overhead windows to characterize the optical quality of these windows. An Air Force tri-bar target was viewed with an 8-in. telescope and a 5-in. telescope for the photographic and visual tests. A Zygo Mark IV interferometer was used for the interferometric tests. Results showed that the windows significantly degraded the performance of both telescopes. At least a 160% degradation in resolution was seen. The results of an independent test conducted by the Armstrong Aerospace Medical Research Laboratory are reviewed and found to corroborate the Aerospace results.

20 DISTRIBUTION/AVAILABILITY OF ABSTRACT	21. ABSTRACT SECURITY CLASSIFICATION	
[X] UNCLASSIFIED/UNLIMITED [X] SAME AS RPT [ ] DTIC USERS	Unclassified	
22a NAME OF RESPONSIBLE INDIVIDUAL	22b TELEPHONE *(Include Area Code)*	22c. OFFICE SYMBOL

CONTENTS

1. INTRODUCTION 5

2. BACKGROUND 7

3. THEORY 9

4. DESCRIPTION OF SHUTTLE OVERHEAD WINDOWS. 11

5. BRIEF DESCRIPTION OF WINDOW TEST 13

6. TEST HARDWARE AND PREPARATION FOR PHOTOGRAPHIC AND VISUAL TESTS. . 15

7. PROCEDURE FOR PHOTOGRAPHIC AND VISUAL TESTS. 17
7.1 Standard Test Run. 18
7.2 Calibration Procedure. 19
7.3 Window Test. 20

8. INTERFEROMETER TEST HARDWARE 23

9. INTERFEROMETER TEST PROCEDURE. 25

10. REVIEW OF RESOLUTION CALCULATIONS. 27
10.1 Theoretical Resolution 27
10.2 Calculating Resolution from Tri-Bar Target Information 29

11. RESULTS OF WINDOW TEST 31
11.1 General Photographic/Visual Results with Two Telescopes. 31
11.2 Specific Meade Results 33
11.3 Specific Celestron Results 34
11.4 Results of the Interferometric Tests 35

12. ARMSTRONG AEROSPACE MEDICAL RESEARCH LABORATORY TEST AND RESULTS. 39

13. SUMMARY OF PHOTOGRAPHIC, VISUAL, AND INTERFEROMETRIC RESULTS . . . 41

14. CONCLUSIONS AND COMMENTS 45

APPENDICES:

A: SPACE SHUTTLE WINDOW LAYOUT A-1
B: PHOTOGRAPHS OF HARDWARE AND TEST SETUPS B-1
C: AIR FORCE TRI-BAR TARGET. C-1
D: AIR FORCE DATA SHEETS D-1
E: MEADE RESULT PHOTOGRAPHS. E-1
F: CELESTRON RESULT PHOTOGRAPHS. F-1
G: INTERFEROMETRIC PICTURES. G-1
H: ORIGINAL ZYGO DATA. H-1

FIGURES

1. Typical Optical System in an Orbiter 9
2. Shuttle Window Layout. 12
3. Dimensions of Overhead Windows 12
4. Hardware Set-up 17
5. Zones in 1723 $AlSiO_3$ Pressure Pane 21
6. Ground-Resolved Distance 28
7. Three-Panes in Shuttle Window Configuration. 36
8. Pressure Pane. 36
9. Redundant Pane 37
10. Fused-Silica Pane. 37
11. Photographic Results 42
12. Visual and Theoretical Results 43
13. Cutoff Point Between Resolving Power and Aberrations 46

TABLES

1. Meade 8-in. f/10 Telescope Resolution Results. 32
2. Celestron 5-in. f/10 Telescope Resolution Results. 32
3. Theoretical Values 33

1. INTRODUCTION

On 1-3 August 1989, the optical quality of the space shuttle overhead windows was tested at the Corning Glassworks plant in Canton, New York. The tests were conducted by Karen P. Scott, David W. Warren, and Michael C. Wanke of The Aerospace Corporation. The tests were in support of the Military Man In Space program and were funded by the U.S. Air Force. The purpose of the tests were to characterize the optical quality of the overhead windows, especially when they are used in conjunction with different aperture telescopes. This report first provides a simple review of the optical theory involved when windows are present in an optical system. Next, a review of the hardware used for the test is presented along with a full procedure on the photographic, visual, and interferometric tests that were conducted. Next, the results are presented with accompanying photographs that were taken during the test. Finally, a review of the tests that were performed concurrently with this test by the Armstrong Aerospace Medical Research Laboratory (AAMRL/HEF) will be presented.

2. BACKGROUND

It has been routine since the first Mercury flight to take photographs and make observations from behind windows in manned space capsules, and the space shuttle has been no exception. Since the first shuttle flight, thousands of pictures have been taken successfully from the shuttle crew cabin through all of the eleven window ports available. The two overhead windows, located behind the pilot and copilot's seats on the upper deck, are the largest of the shuttle windows and the most widely used since they typically face earthward most of the time. Although there has been unequivocal success taking photographs with small aperture optical systems (on the order of an inch), the ability of the windows to support observations with medium to large aperture optical systems was unknown. The interferometric, visual, and photographic tests conducted and described in this report do prove that the standard shuttle windows (excluding the high-optical-quality hatch window) are not of sufficient quality to support medium aperture optical system observations.

3. THEORY

The shuttle windows are the first optical element to any optical system (camera, telescope, radiometer, etc.) used in the shuttle crew cabin. Depending on the optical system used, the windows can have a serious effect on the amount and quality of information obtained for a particular experiment. The windows "effect" can be described in terms of the aberrations induced on the initial optical wavefront that enters the system after it passes through the window.

Figure 1 illustrates a typical imaging system located in the crew cabin of an Orbiter. The optical system could be a telescope or a camera.

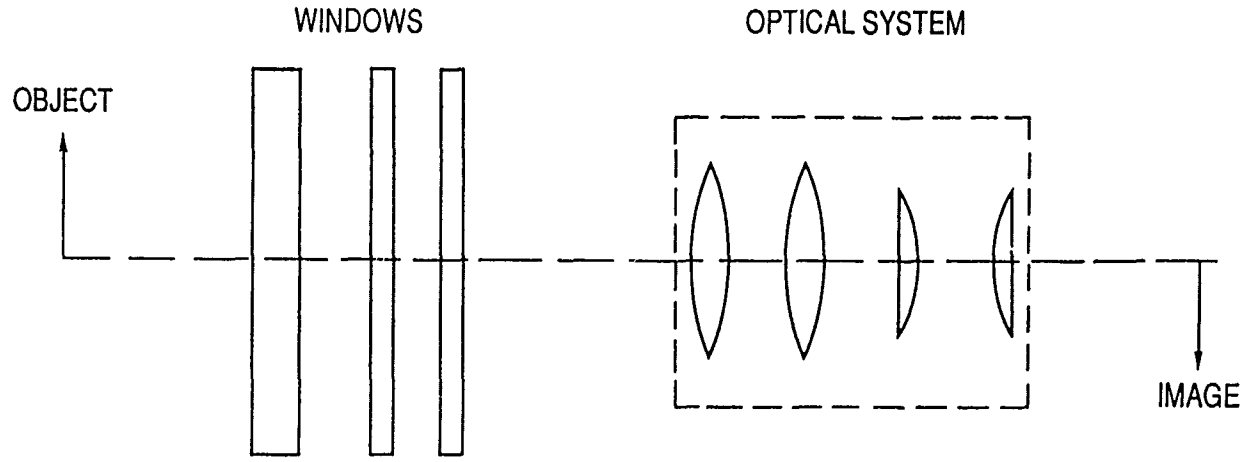

Figure 1. Typical Optical System in an Orbiter

An ideal window needs to be homogeneous. Errors occur if the light has not traveled the same optical path due to either surface errors or index of refraction variations in the glass (the glass is not homogeneous). Aberrations typically increase proportionally to the area of glass traversed. This is why window quality can become an issue when large diameter telescopes are used but with the same window can be insignificant when smaller diameter telescopes or cameras are used. For a much more complete discussion of this subject, see Reference 1.

[1]Scott, Karen P., "Basic Theory of Designing Optical Quality Spacecraft Windows," Report No. TOR-0091(6508-21)-2, The Aerospace Corporation, El Segundo, CA, August 1991.

4. DESCRIPTION OF SHUTTLE OVERHEAD WINDOWS

The shuttle overhead window configuration consists of a three-pane system. Figure 2 illustrates the window composition of the three panes and their positions with respect to each other. The approximate dimensions of the windows are given in Figure 3. A copy of the Space Shuttle Window Layout can be found in Appendix A. The layout was taken from Rockwell International Document #MC 332-0006 in which the window group numbers are listed. The three overhead windows consist of the following materials and coatings: (a) the thermal or outside window consists of 7940 fused silica and is uncoated (Window #0029); (b) the middle or "redundant" pane (Window #0020) is made of 1723 $AlSiO_3$ (alumina silicate) and is a tempered pane that absorbs in the ultraviolet (UV), and it is coated with a high-efficiency, anti-reflection (HEA) coating on both sides; (c) the "pressure" pane (Window #0021) located in the crew cabin also is composed of 1723 $AlSiO_3$ and is coated with HEA and a red reflector (to reflect infrared). It is the $AlSiO_3$ panes, not the coatings, that shield the astronauts from the harmful UV radiation. The HEA coating reduces the usual 4% fresnel loss per surface in the visible spectrum, and the red reflector shields the astronauts from harmful infrared radiation. The approximate dimensions of the windows are given in Figure 3.

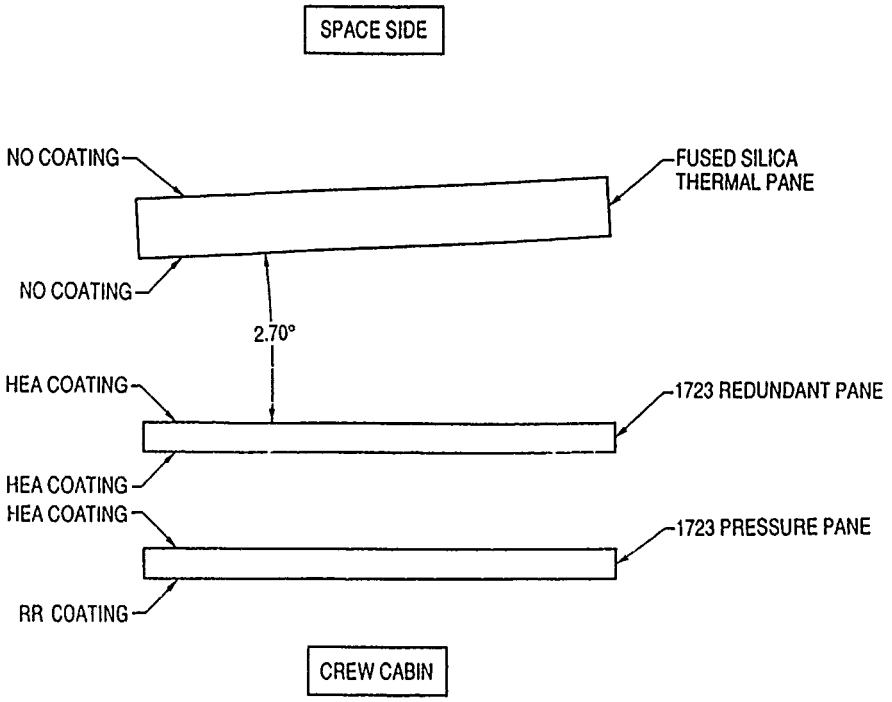

Figure 2. Shuttle Window Layout

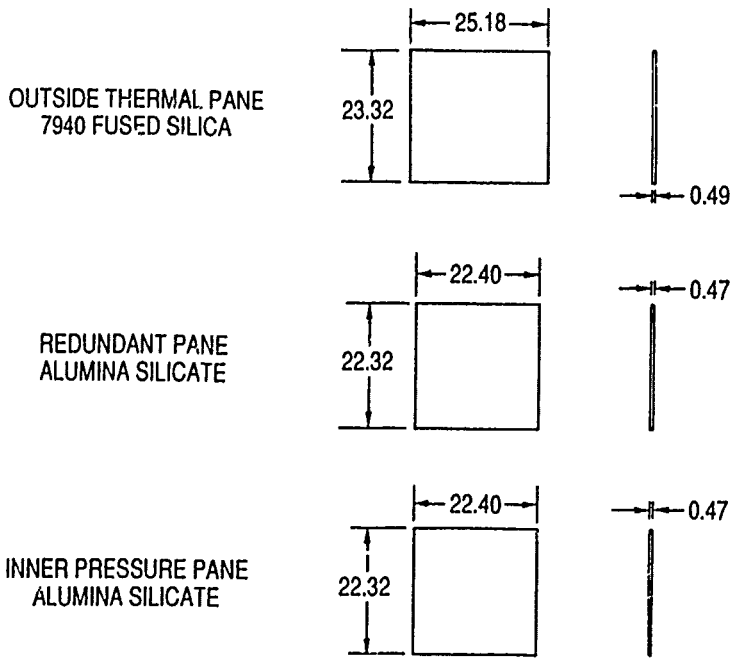

Figure 3. Dimensions of Overhead Windows

5. BRIEF DESCRIPTION OF WINDOW TEST

The Aerospace test was composed of two different parts: (a) an interferometric test with a Zygo Mark IV interferometer and (b) a photographic and visual test with an 8-in. aperture Meade telescope and a 5-in. aperture Celestron telescope. For both parts of the test, the windows were installed in a custom mount designed and constructed by Corning. The mount consisted of a wooden frame with slots positioned to approximate shuttle window configuration. The mount worked very well and was found not to introduce any stress on the windows (Photographs 1 and 2, Appendix B). All windows were tested individually and in shuttle window configuration during each part of the test.

The interferometric test was conducted to obtain an overall idea of the quality of the windows over different apertures and to measure the wavefront errors present for different aberrations. A video of the interferograms was made as the Zygo was scanned around the windows. It was found to be impossible to study the windows over any aperture larger than about 4 to 5 in. because of the poor quality of the windows.

The visual and photographic tests with the two telescopes were performed to determine the amount of degradation the windows induced when one views through them. The telescopes first were calibrated by viewing a standard Air Force tri-bar target (see Appendix C) with no windows present. Next, the windows were placed in the optical path, and differences induced by the windows were recorded both photographically and visually. A more detailed description of the procedure is presented in Section 6.

6. TEST HARDWARE AND PREPARATION FOR PHOTOGRAPHIC AND VISUAL TESTS

The hardware preparation for the photographic and visual tests with the Celestron and Meade telescopes took careful thought and extensive pretest experimentation. The two most serious problems were focus errors and vibration. The following hardware list was developed over many iterations to meet the challenge of these problems.

The test hardware comprised four major assemblies as follows: (a) Meade, (b) Celestron, (c) photographic, and (d) target assemblies.

a. Meade assembly:
- Meade f/10 8-in. telescope
- Large Quickset tripod
- Two mounting posts
- Eyepiece holder
- Two eyepieces: Meade 25 mm
  Super Plossl 6.4 mm
- Two nylon straps
- Configured aluminum plate
- Four C-clamps
- Foam padding and sandbags

The Meade telescope was attached to two posts mounted on a large aluminum plate which, in turn, was attached to the tripod and secured with four C-clamps. The foam padding, sandbags, and straps were used to secure the front of the telescope and reduce vibration (Photographs 2 and 3, Appendix B). The 6.4-mm and 25-mm eyepieces were used for the visual test.

b. Celestron assembly:
- Celestron f/10 5-in. telescope
- Mounting stage
- Tripod (same as above)
- Eyepiece holder
- Configured aluminum plate
- Two eyepieces (as listed above)

The Celestron telescope was mounted in a small cradle which, in turn, was mounted on the stage that stood on the aluminum plate that attached to the tripod with four C-clamps (Photograph 4, Appendix B).

c. Photographic assembly: 35mm Nikon F3 camera
One standard camera back
One modified camera back
One shutter cable for Nikon
Two T-mounts
Uniblitz model SD 1000 shutter
Microscope: 55-mm Nikor lens
Focusing stage
Eyepiece holder
25-mm eyepiece
Three Oriel slides with posts
Kodak 2415 film

The photographic assembly probably was the most complicated (Photographs 5 and 6, Appendix B). As will be explained in Section 6, focusing the telescope to the camera was very difficult. It was found that a microscope was needed so that the telescope could be focused directly onto the film plane. The Nikon viewer assembly, even when a ground glass focusing screen was used, was found to be too inaccurate to use for focusing the telescope image onto the film plane. The main problem was the slightly inaccurate placement of the 45° fold mirror which directs the image to the focusing screen or view finder at the top of the camera (we found this problem in all the cameras tested).

An external shutter also was used instead of the internal camera shutter because of vibration problems. It was found that the motion of the camera shutter during an exposure was enough to cause degradation in the resulting photograph (a double image in the horizontal direction). The external shutter had an iris diaphragm with exposure times controllable to 0.1 msec. It was found to be a good addition, since it induced no vibration problems. The entire assembly--including the microscope, camera, and shutter--was attached and mounted on posts to form a single unit that could be translated along the Oriel slide and attached to the telescope back via a T-adapter.

d. Target assembly: Standard Air Force glass tri-bar target
2x2-in. opal diffuser
60-W lightbulb
Oriel slide
Medium-sized tripod

A glass tri-bar target was selected so that back illumination could be utilized. The opal diffuser was placed between the 60-W bulb and the tri-bar target to ensure uniform illumination. (It was found to be difficult to achieve uniform illumination when using a plain tri-bar target photograph and external lighting.) The whole tri-bar target assembly was mounted on an Oriel slide, so it could be translated as part of the focusing procedure (see Section 6 and Photographs 7 and 8, Appendix B).

7. PROCEDURE FOR PHOTOGRAPHIC AND VISUAL TESTS

The purpose of this part of the test was to determine the degradation that the windows introduce when a medium-to-high resolution telescope is used to view through them. This test was separated into two parts: (a) a calibration with the telescope only and (b) a test with telescope and windows. The results then could be compared, therefore determining the degrading effects caused by the window being in the optical path of the telescope.

This part of the test was conducted in 117 ft of a 300-ft hallway in the Canton plant (Photograph 9, Appendix B. Figure 4 illustrates the basic hardware set-up.

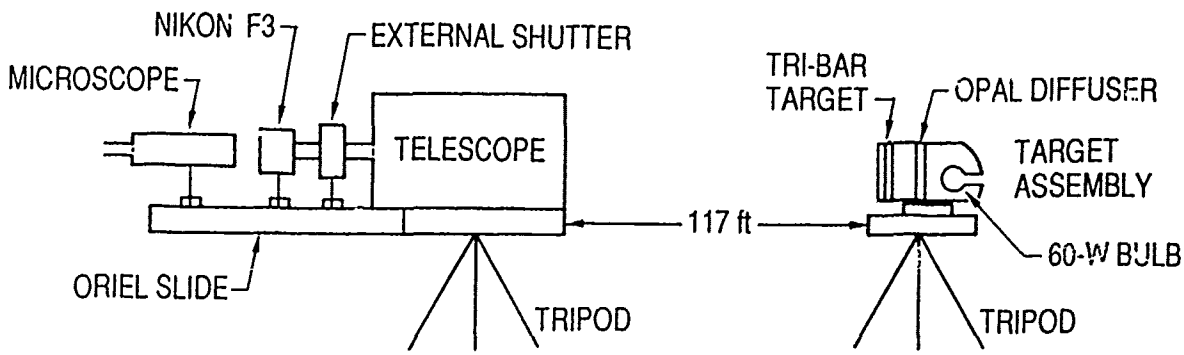

Figure 4. Hardware Set-up

The plant was on official shutdown, so much of the heavy air-handling equipment was turned off. Some of the nearby air-conditioning ducts also were turned off upon request. All of the photographic tests were conducted after hours, between 7 p.m. and 4 a.m., when most of the Corning personnel were gone. Every effort was made to reduce vibration and air turbulence in the test area.

7.1 STANDARD TEST RUN

A description of a "standard" run is listed below. This standard procedure was followed for either a calibration or a window run.

a. Exposure Time: The optimal exposure time was determined once at the beginning of the test. Several exposure runs were conducted and the film developed at the site. It was determined that a 1.8 msec exposure time was optimal; this time was used for the remainder of the tests.

b. Visual Test: The visual test was conducted first to locate the target in the telescope field of view (FOV) using the 25-mm eyepiece. After this was accomplished, the 6.4-mm eyepiece (higher magnification) was used to determine visual resolution by noting the target group that could be resolved (Example: Group 3^1 which means Group 3, Element 1).

c. Focusing for the Nikon: This part of the test was one of the most difficult. The problem is that film is very sensitive to focus errors (defocus), and the eye is very good at accommodating for defocus. Hence, when your eye is focusing on a target, it will change to remove slight errors so that the target can "look" in focus when actually it is slightly off. The effect of a slightly defocused image on film is a moderate-to-severe degradation in resolution. The solution to this problem was not to rely on the eye for focus but instead to take a systematic through-focus run. The through-focus run was achieved by moving the target assembly a total of 17 cm which resulted in a focus shift at the film plane of approximately 13 thousandths. This was found to be adequate to correct the eye errors.

   The full focus procedure consisted of first mounting the modified camera back onto the Nikon camera. The modified back had a hole drilled in it, so the film plane could be viewed with the microscope. The film plane was established by a piece of transparent film (with a fine crosshair exposed on it) that was attached to the camera back and placed so that, upon closing the back, the film would simulate real film in the camera. Next, the microscope was focused on the crosshair on the film. The image of the target then was brought into focus by adjusting the telescope. To reduce the accommodation of the eye, one would first focus on the crosshair, then (to look for parallax) scan quickly back and forth between the crosshair and the target until they appeared to be in the same focus. During focusing, the camera was set on bulb and the external shutter was set open.

d. Preparing the Camera: After focusing was complete, the modified back was taken off and replaced with the standard back. Next, the external shutter and the camera shutter were closed. Kodak 2415 film then was loaded and the back closed. At this point, focus cannot be checked until the end of the run when the film is unloaded.

e. Taking Pictures: The target was focused with it located at the middle of its range (9-cm mark) on the Oriel slide. After the first picture was taken, the target moved in 0.5-cm steps along the Oriel slide from 9-17 cm to 8.5-0.0 cm. A total of 34 pictures were taken for each run. After development, a few well-focused exposures always were guaranteed.

Descriptions of the calibration and window test procedures are provided below.

7.2 CALIBRATION PROCEDURE

The same calibration test was conducted for both telescopes. Beyond determining the optical quality of the telescopes, the calibration runs also allowed analysis of the vibration and air turbulence induced by the surrounding environment. Low-level vibration does not affect the visual tests, because the eye will accommodate for it. However, film is not forgiving at all and, due to the long focal lengths of the telescopes, the test assemblies were highly sensitive to vibration. The effects of vibration are seen in photographs as a reduction in resolution.

Several calibration runs were conducted so that some of the rolls could be developed on site for comparison of previous results from pretest at The Aerospace Corporation, while others could be developed later at more controlled developing facilities. A source of constant temperature water was not available (especially for rinse) at the Canton plant. However, the developing was good enough for preliminary information. Upon developing the film on site, we found that the facility had a slightly worse vibration problem than in the pretest runs conducted at Aerospace, but the results were close; this proved that the current test area would be adequate for the window test.

7.3 WINDOW TEST

For this part of the test, all windows were tested individually, then in shuttle window configuration with both telescopes. The window test was much more complicated than the calibration test because of the severity at which the windows degraded the telescope images. The variation in focus over any particular field of view made focusing on the target difficult. In particular, the 8-in. telescope was very difficult to use, because there was no one focus to be found due to severe astigmatism and multiple overlapping "ghost" images. These problems will be discussed further in Section 10. For the Meade test, a change was made in the through-focus run procedure because of the large focus variation; it was found that just moving the target was not adequate to meet this large variation. Hence, for the Meade, a modified through-focus run was developed in which the focus knob on the Meade was adjusted by even increments to cover the range. Significant points were noted such as best horizontal focus, best vertical focus, best average focus, and a few other points. Photographs were taken of these points and are presented in Subsection 11.2. This procedure was not necessary for the Celestron, because the standard focus shift provided by the Oriel slide was sufficient to explore the presence of the window degradation.

During the Celestron part of the test, it was discovered that all the individual windows were highly variable in quality, depending on which area of the window was being viewed. This was discovered when the effect of viewing angles on image quality was being tested. It was found that there was no consistent effect from changing the viewing angle, but there was a huge effect in changing the viewing area. In other words, there were good and bad zones in each window (changing the angle of the window had the effect of moderately changing the viewing area). For example, on the 1723 pressure pane, there are two tong marks at one end from the tempering process in fabrication (see Figure 5). It was found that at the opposite end from the tong marks, the image quality was very good (Group 2^3). When the Celestron was moved to the center of the window, the image degraded to a Group 1^6. Finally, when the Celestron was moved to the end of the window between the tong marks, the image

quality degraded to its worst point with many overlapping images and a resolution not even in Group 0! If one was observing through these windows at a 190-nmi orbit, this would correspond to a resolution degradation that would go from 8.1 ft to 9.1 ft to 36 ft depending on the area of the window being viewed. Surprisingly, the fused-silica window also was equally variable, even though it had not gone through a tempering process like the other windows.

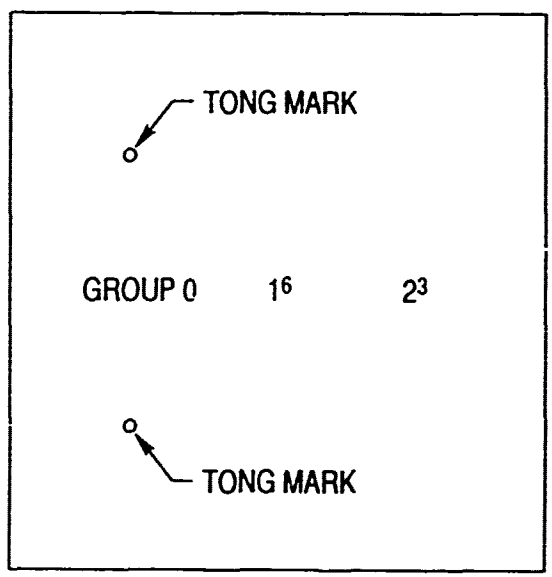

Figure 5. Zones in 1723 $AlSiO_3$ Pressure Pane

8. INTERFEROMETER TEST HARDWARE

An interferometer is used to test, to a very high accuracy, the wavefront transmitted or reflected from an optical component (a window or mirror). By analyzing the wavefront, one can determine the quality of an optical component. In this test, the interferometer measured the effects of surface errors and inhomogeneity in the windows and, therefore, the image quality that could be expected when viewing through the windows.

Corning provided all the hardware for the interferometric test which included:

a. 18-in. aperture Zygo Mark IV interferometer
b. 18-in. reference flat (good to $\lambda/2$ at λ = 632.8 nm over 18 in.)
c. Standard optical table and isolated environment
d. Phase-shifting software for interferometric analysis
e. Window mounting jig
f. Video equipment and microphone

The test took place in an isolated room with constant temperature control (Photographs 10 and 11, Appendix B). An outside control room was used to manipulate the interferometer and observe the wavefront characteristics on a monitor.

9. INTERFEROMETER TEST PROCEDURE

The windows were tested individually and then in shuttle window configuration by looking at the transmitted wave bouncing off the flat and returning into the phase-shifting interferometer. The software corrected for the double pass through the window. None of the windows could be tested over more than a 5-in. aperture area because of the poor quality of the windows (the number of fringes became too great). What became noticeable immediately when we tested the individual windows was the large, moving bulls-eye as we scanned around the aperture. The bulls-eye corresponded to a bow in the window which was inducing a defocus error in the wavefront of approximately four waves over a 4-in. aperture. This effect was seen in all three windows and was not caused by the mount (we tested this hypothesis by loosening the mount completely until the window was just leaning against it). All the windows had bad edge areas. The fused-silica pane displayed bad astigmatism on two sides. Other results will be described in Subsection 11.4.

It was found that the windows were of too poor a quality to accurately map the zones. Instead, a video was taken that effectively illustrated the variation in the windows by scanning the Zygo around different parts of each window or windows being tested. Photographs also were taken of individual areas.

10. REVIEW OF RESOLUTION CALCULATIONS

The purpose of this section is to review some of the key calculations that will be presented in Section 11. In order to compare the performances of the Celestron and Meade systems, the resolution numbers are converted into the ground resolution capability that would be expected at a typical Orbiter altitude of 190 nmi. The ground resolved distance (GRD) is the minimum distance that two 100% contrast objects (e.g., search lights on a black background) could be apart and still be resolved. In the photographic tests, a 100% contrast image was used. Remember that resolution is sensitive to and depends on a number of things including: (a) object contrast, (b) motion or vibration of the optics, (c) focal plane resolution capabilities, and (d) diameter of the optics. The Corning test was nearly ideal in that vibration and air turbulence were minimal; hence, the resolution test results should be regarded as nearly ideal. If these results are applied to another environment such as the Orbiter, the quality of the optical environment must be considered. If it is not ideal, the test results will not scale accurately.

10.1 THEORETICAL RESOLUTION

The ultimate limitation on resolution, if everything else is perfect, is determined by the diameter of the optics. The theoretical resolution that is presented in Section 11 is determined using the Rayleigh criterion

$$\theta_r = 1.22\lambda/D \text{ rad}$$

where λ = wavelength, D = diameter, and

$$GRD = R\theta_r$$

where GRD = ground-resolved distance and R = target range. As an example, for the 8-in. diameter Meade (203-mm) telescope, the theoretical resolution calculated for a target range of 190 nmi would be as follows if the windows were ideal:

$$\theta_r = \frac{(1.22)\ (5 \times 10^{-4}\ \text{mm})}{203\ \text{mm}}$$

$$= 3 \times 10^{-6}\ \text{rad}$$

$$R = (190\ \text{nmi})(1.15\ \text{stat.m/nmi})(5280\ \text{ft/stat.m})$$

$$= 1{,}153{,}680\ \text{ft}$$

$$GRD = R\theta_r = 3.5\ \text{ft}$$

Hence, if the windows were ideal, the telescope optics were ideal, the vibration were minimal, and objects were in a 100% contrast condition, the Meade telescope would be able to resolve two points that were 3.5 ft apart (see Figure 6).

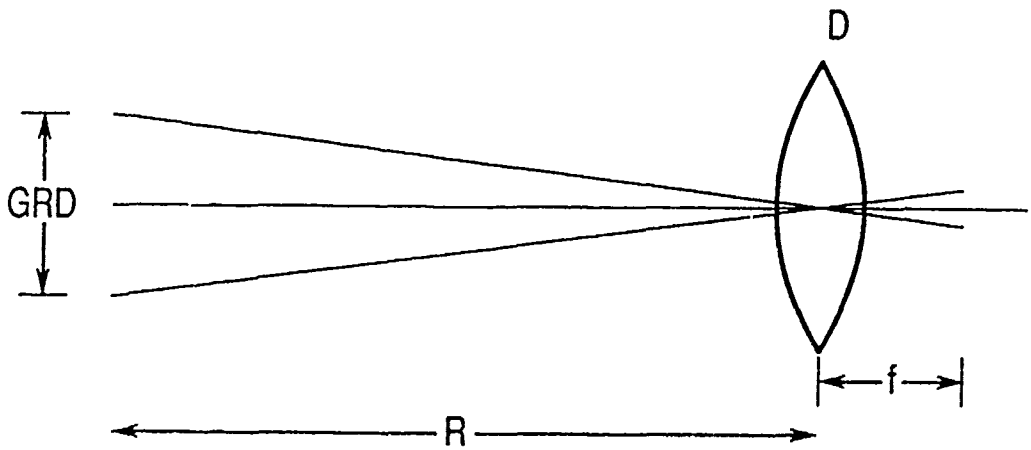

Figure 6. Ground-Resolved Distance

10.2 CALCULATING RESOLUTION FROM TRI-BAR TARGET INFORMATION

The purpose of the Corning test was to determine the effect of the shuttle windows on the actual resolution capabilities of different aperture telescopes. The standard Air Force tri-bar target (as shown in Appendix C) and the Air Force tri-bar data reduction sheet (see Appendix D) was the method used to determine resolution capability. The general idea is that if the resolution capability can be determined at one target range, then this information can be used to determine the expected resolution capabilities at different ranges such as at 190 nmi.

For example, during the Corning test, Group 2, Element 4 was the smallest pattern from the tri-bar target (117 ft away) that could be observed visually with the Celestron with no windows present. In Appendix D under Group 2, Element 4, it states that this pattern corresponds to 5.6988 lines/mm. That means that 5.6988 lines (one line corresponds to one dark line and one space, or the center-to-center distance between two adjacent dark lines) will fit in 1 mm or, more importantly, the center-to-center distance between two adjacent dark lines is 1/5.6988 or 0.175 mm. From this, a GRD at 190 nmi can be calculated.

$$\tan\theta = \frac{(0.175 \text{ mm})}{(117 \text{ ft} \times 12 \text{ in./ft} \times 25.4 \text{ mm/in.})}$$

$$= 4.92 \times 10^{-6} \text{ rad}$$

$$\text{GRD} = R\tan\theta$$

$$= (1{,}153{,}680 \text{ ft}) \times (4.92 \times 10^{-6} \text{ rad})$$

$$= 5.68 \text{ ft}$$

11. RESULTS OF WINDOW TEST

11.1 GENERAL PHOTOGRAPHIC/VISUAL RESULTS WITH TWO TELESCOPES

Tables 1 and 2 illustrate the visual and photographic test results from the Meade and Celestron tests. As expected, the natural reduction in resolution is apparent between the visual and photographic tests. The criteria used to determine the resolution results for both the visual and photographic tests were as follows: (a) both sides of the FOV had to be resolved (both adjacent tri-bar targets), (b) both vertical and horizontal patterns had to be resolved (i.e., the criterion did not allow resolution of horizontal lines while the adjacent vertical lines were washed out denoting astigmatism), (c) the higher frequencies associated with anomalous resolution (where resolution washes out at middle frequencies but then partly returns at limited higher frequencies in highly aberrated systems) also were not considered. All photographic resolution numbers were determined from the photographic negatives.

The windows were highly variable, but generally the results listed in the table represent resolution values taken from the center of the window and should be considered average values for that window system. Numbers that are marked with a double asterisk should be considered carefully, since they denote poor overall image quality. When results are compared between the Meade and Celestron telescopes, only the GRD numbers should be used. Table 3 lists the absolute theoretical resolution limits of the Celestron as determined using the Rayleigh criterion.

Table 1. Meade 8-in. f/10 Telescope Resolution Results

Visual/Photo	Windows	Group	GRD(190 nmi)	Run/Photo No.
1. Visual	NO	3^1	4.0 ft	2
2. Visual	Three panes	1^6	9.1*	11
3. Visual	Pressure	1^6	9 1	8a
4. Visual	Redundant	1^6	9.1	8b
5. Visual	Fused silica	1^6-2^4	5.7-9.1*	9
6. Photo	NO	1^6-2^1	8.1-9.1	10-30a
7. Photo	Three panes	-1^6-0^2	28.8-36.3*	1i-12a,15a,18a,21a,24a
8. Photo	Pressure	0^6	18.2	8a-27a
9. Photo	Fused silica	1^3	12.7	9-28a

Table 2. Celestron 5-in. f/10 Telescope Resolution Results

Visual/Photo	Windows	Group	GRD (190 nmi)	Run/Photo No.
1. Visual	NO	2^4	5.7 ft	12
2. Visual	Three panes	1^6-2^1	8.1-9.1*	12
3. Visual	Pressure	1^6-2^3	6.4-9.1	14
4. Visual	Fused silica	2^1-2^3	6.4-8.1	15
5. Photo	NO	1^6	9.1	13-6a
6. Photo	Three panes	-1^6-0^2	28.2-36.3*	12-25a
7. Photo	Pressure	0^1	32	14-26a
8. Photo	Fused silica	0^5	20.4	15-9a,11a

*Stands for very poor quality images, inconsistent resolution across the FOV, and overlapping ghost images

Table 3. Theoretical Values

Telescope	GRD (190 nmi)
1. Meade	3.5 ft
2. Celestron	5.5 ft

As seen in Tables 1 through 3, the shuttle overhead windows significantly decreased the optical performance of both telescopes. Without the windows in place, nearly diffraction-limited performance was achieved for both telescopes. This is apparent when we compare the visual GRD results with the calculations in Table 3. With the full three panes in place in shuttle window configuration, moderate to severe astigmatism and overlapping ghost images were seen with both telescopes. The photographic results indicate that not all vibration was eliminated from the Meade setup since, theoretically, the Meade should produce better resolution results than the Celestron. Overall, however, the photographs are more than satisfactory to illustrate the poor optical quality of the overhead shuttle windows (see Section 13 for a summary of all photographic and visual results).

11.2 SPECIFIC MEADE RESULTS

Tables 1 through 3 indicate that the three-pane shuttle window port caused a reduction in resolution of at least 200% when used with the Meade telescope. Problems with focusing the Meade when viewing through the three-pane configuration have been discussed several times in this report. Five photographs of the modified through-focus run (described in Subsection 7.3) are provided to illustrate the severe astigmatism observed. The photograph numbers and key points that each picture displays are listed below (see Appendix E):

a. Reference photograph (no windows), 10-30a

b. Best vertical focus, washed out horizontal focus (three panes), 11-15a

c. Better horizontal focus, worsening vertical focus, 11-18a

d. Best focus for horizontal and vertical together, 11-21a

e. Best horizontal focus, lousy vertical focus (also shows the checkerboard pattern that was seen often), 11-24a.

The variability in the horizontal and vertical foci indicates severe astigmatism. The variability of quality within the same FOV also is obvious with these pictures. In Photograph 11-21a (Appendix E), the left side of the FOV has a reasonable focus for the horizontal elements; but on the right side, both horizontal and vertical elements are washed out.

11.3 SPECIFIC CELESTRON RESULTS

The Celestron saw fewer aberrations induced by the window due to the smaller aperture. Optical aberrations (spherical, coma, astigmatism, etc.) are aperture dependent; they go by at least the square of the aperture size depending on the type of aberration. The Celestron results were better with a reduction in ghost images and astigmatism, but both effects still were evident. A reduction in resolution of 160 to 360% was seen with the Celestron telescope. However, there was less variability across a given FOV, so an overall image was less confusing (see Appendix F). The windows still are variable, even with the Celestron, to the point that scanning the telescope across the good and bad zones in the shuttle probably still would result in confusing images. However, if one consistently could stay away from the area where the tong marks (physical marks on the $AlSO_3$ windows) are located, the Celestron might be useable (if one need not scan the telescope). Finally, in the photographs, a marked reduction in contrast which affects resolution also was seen. Hence, even though the Celestron yielded better results, the instrument probably would yield only marginal results if used in the shuttle.

11.4 RESULTS OF THE INTERFEROMETRIC TESTS

A 1.5-hr video was made of the interferometric tests. Specifically, the video shows the resulting interference patterns as the Zygo Mark IV interferometer was scanned around different areas of individual windows and with all windows in shuttle window configuration. In addition, photographs of key areas were taken and are included in Appendix G of this report.

Phase-shifting hardware was used to measure aberrations in the different areas of each individual window as well as in the three-pane configuration. Analytically, only 1- to 5-in. diameter areas could be measured with the phase-shifting software (depending on the zone and number of windows) because of the poor optical quality of the windows. Figures 7 through 10 show general maps of the center 18-in. areas (the largest aperture that could be looked at by the Zygo) of the individual windows and the three panes together. Photograph numbers of the specific areas are given to the right and are located in Appendix G. The windows are oriented so the tong marks are on the left as they were in the pictures. The pressure pane was of the worst quality of the three panes, especially at the edges. The fused-silica pane had a severe astigmatism component that was particularly obvious near two of the edges. The collected aberration information for the centers of the windows is included next to each figure, with the reference wavelength being $\lambda = 632.8$ nm. The numbers cannot be compared directly, because different diameter test areas were measured and aberrations are very aperture dependent. The purpose for listing the aberrations is to give a general idea of the optical quality of all the individual windows. Copies of the original data sheets are located in Appendix H.

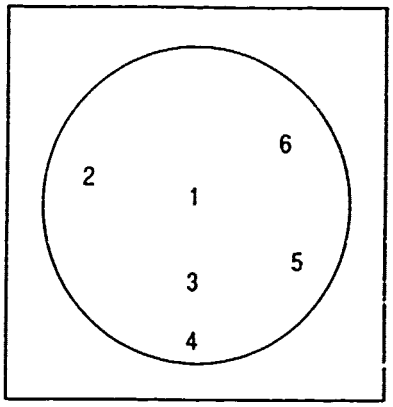

Photograph Nos.

1. 2-32
2. 2-34
3. 2-35
4. 3-1
5. 3-3
6. 3-6

Center of Window

Diameter tested: 4.5 in.
P-V: 1.160
rms: 0.221
Power: 4.1113
Astigmatism: 0.9299
Coma: 1.2705
Spherical: 0.6174

Figure 7. Three Panes in Shuttle Window Configuration

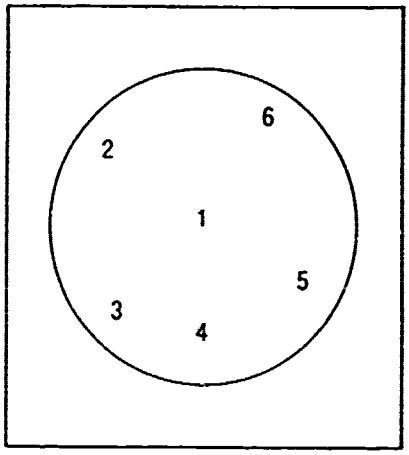

Photograph Nos.

1. 3-7
2. 3-11
3. 3-14
4. 3-16
5. 3-17
6. 3-20

Center of Window

Diameter tested: 5.5 in.
P-V: 2.017
rms: 0.304
Power: 5.1600

Figure 8. Pressure Pane

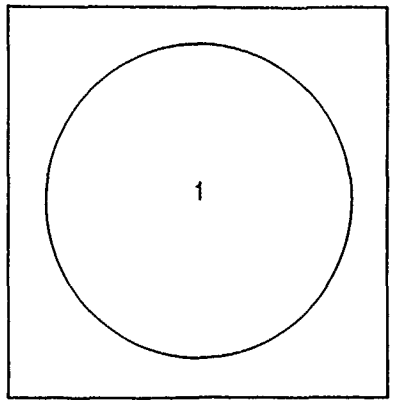

Photograph No.

1. 3-23

Center of Window

Diameter tested: 3.5 in.
P-V: 1.532
rms: 0.281
Power: 3.1361
Astigmatism: 1.6035
Coma: 0.2472

Figure 9. Redundant Pane

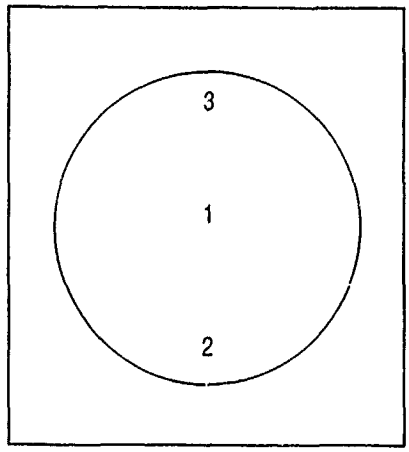

Photograph Nos.

1. 3-30
2. 3-33
3. 3-36

Center of Window

Diameter tested: 3.0 in.
P-V: 0.629
rms: 0.113
Power: 2.3155
Astigmatism: 0.6498
Coma: 0.0787

Figure 10. Fused-Silica Pane

12. ARMSTRONG AEROSPACE MEDICAL RESEARCH LABORATORY TEST AND RESULTS

The tests performed in concurrence with the Aerospace tests were performed by personnel from the Armstrong Aerospace Medical Research Laboratory (AAMRL/HEF). The following review has been taken from the final report (see Reference 2). The purpose of the test was to determine the effect of the overhead windows on the resolution of the Spaceborne Direct-View Optical System (SpaDVOS) optics. Specifically, a Vivitar telephoto zoom, 120- to 600-mm focal length, f/5.6 lens was used for both visual and photographic tests (Photographs 12 and 13, Appendix B). Eighteen different aperture sizes were tested in combination with three focal lengths (120 mm, 300 mm, and 600 mm). The range of aperture sizes tested was from 0.15 to 2.95 in.; the windows were tested at normal incidence and at 30° off normal. Only the central areas of the windows were tested. The results from the test are as follows:

a. Resolution increased with aperture size at all focal lengths.

b. At the shorter focal lengths (120 mm and 300 mm) where the aperture size ranged from 0.15 to 2.11 in., there was no statistically significant degradation in resolution.

c. Statistically significant resolution degradation was found for the 600-mm focal length at apertures of 2.15 and 2.95 in. tested at 30° off normal.

d. Generally, at apertures larger than approximately 2 in., the wavefront distortion effects due to the window are comparable to the diffraction effects of the objective lens.

e. The condition for which maximum resolution was achieved through the window assembly was with the 600-mm focal length and an aperture of 2.95 in. (f/8). At a 160-nmi orbit, this would correspond to a ground resolved resolution of 9.0 ft. Without the window, 8.0 ft would be expected. A moderate degradation in resolution is induced by the window assembly.

[2]Merkel, Harold S. and Harry L. Task, "Optical Test of the Space Shuttle Overhead Windows," Report No. AAMRL-TR-90-024, Harry G. Armstrong Aerospace Medical Research Laboratory, Human Systems Division, Air Force Systems Command, Wright-Patterson Air Force Base, Ohio, May 1990.

13. SUMMARY OF PHOTOGRAPHIC, VISUAL, AND INTERFEROMETRIC RESULTS

Figures 11 and 12 show the combined visual and photographic results of the AAMRL and Aerospace tests. The figures are intended to show general trends rather than exact numbers, since there was significant variation in window quality and in the data. The results (shown in the figures) represent averages obtained from the data. For the AAMRL photographic data, a 100% decrease from the visual data was assumed, since the data varied significantly (i.e., if one achieved a maximum visual resolution of 13 ft, then a maximum photographic resolution of 26 ft is assumed). The theoretical data are calculated using the Rayleigh criterion. The GRD axis assumes a 190-nmi orbit for comparison (as discussed in Section 10).

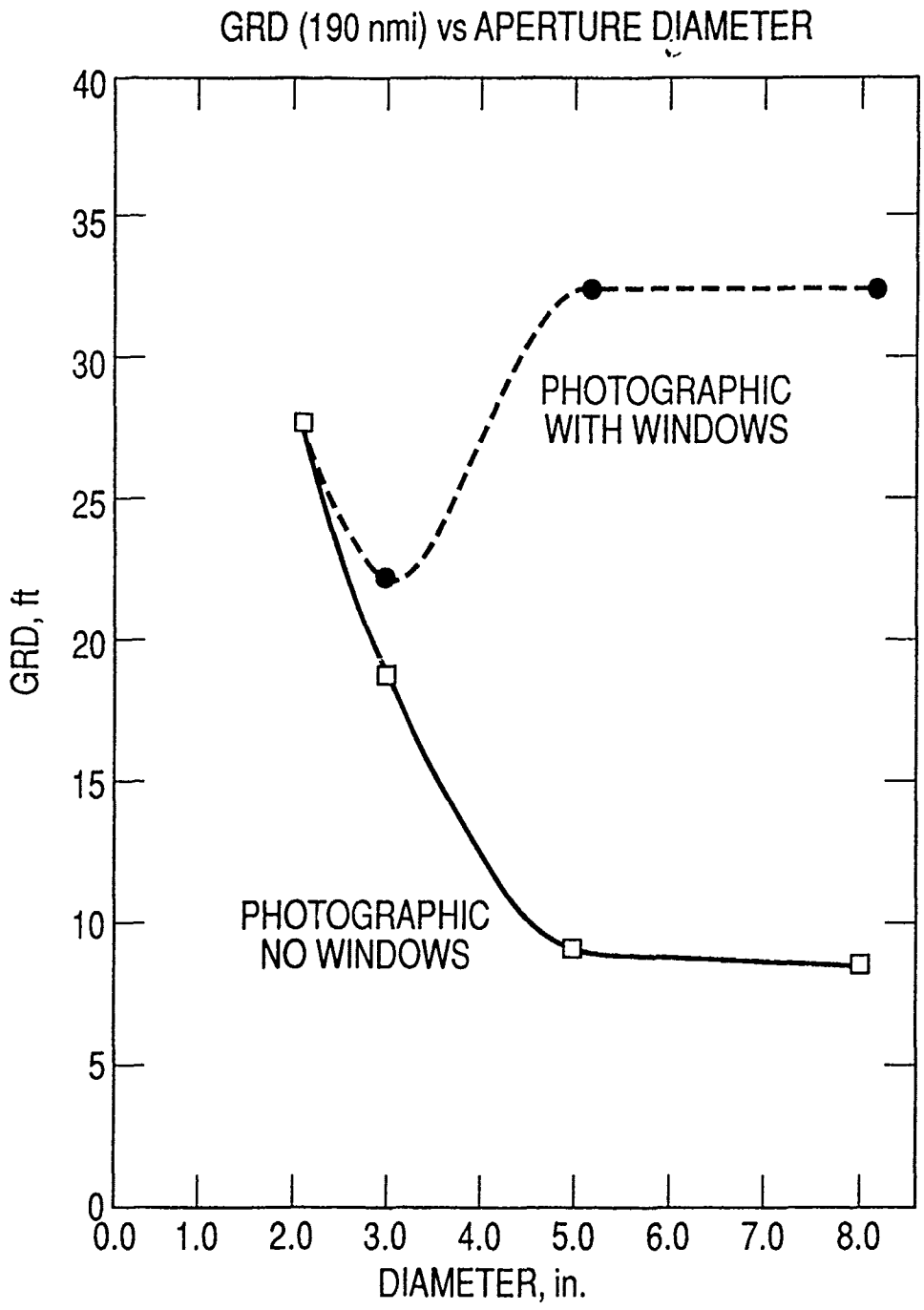

Figure 11. Photographic Results

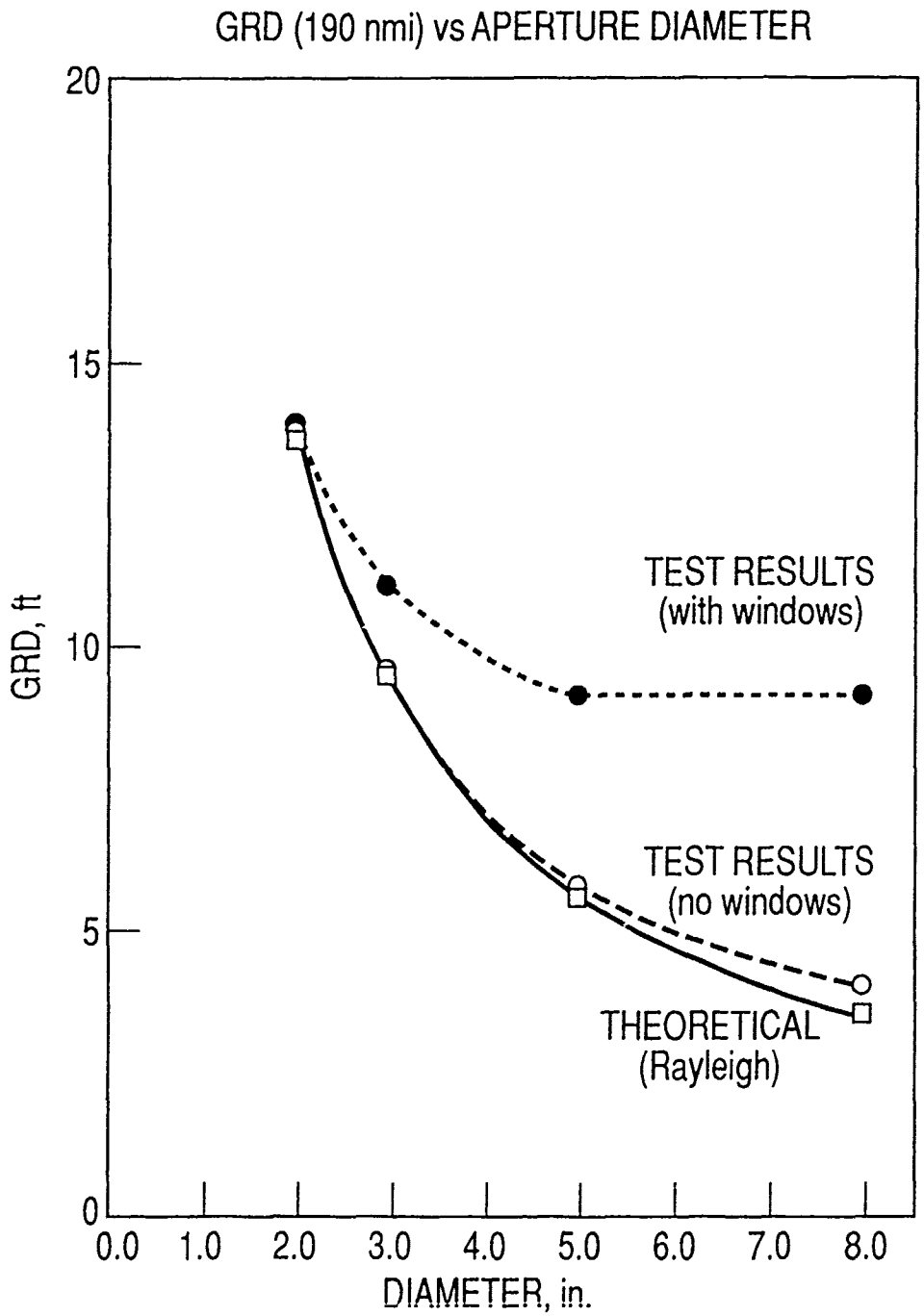

Figure 12. Visual and Theoretical Results

From Figures 11 and 12 as well as other discussions in this report, the following results are clear:

a. Resolution increased with aperture size when the windows were not present.

b. Nearly diffraction-limited performance was achieved with both telescopes when the windows were not present.

c. With the three-pane shuttle window assembly in place, the maximum resolution of the 8-in. Meade telescope decreased 200 to 400%.

d. With the shuttle window assembly in place, the resolution of the 5-in. Celestron telescope decreased 160 to 360%.

e. The quality of the images for both telescopes was affected detrimentally beyond the resolution loss with an increase in ghost images, increased difficulty in focussing, lost contrast, and prevalent astigmatism as seen in the photographs in Appendices E and F.

f. Window quality varied tremendously, especially in the $AlSiO_3$ windows. The side away from the tong marks (physical marks on the windows where they hold the windows during the tempering process) was of better optical quality then the side near the tong marks.

g. The interferometric test results agree with the photographic and visual results. The test results indicate a significant amount (one to four waves over 3- to 5-in. apertures) of aberrations present in all of the windows. In particular, all the windows were bowed, introducing a large power term (not a problem for telescopes) and a large amount of astigmatism in the fused-silica window.

14. CONCLUSIONS AND COMMENTS

This report has described the visual, photographic, and interferometric tests conducted on an unused spare set of shuttle overhead windows. The tests have made it clear that the shuttle overhead windows were not designed to be used in conjunction with medium aperture telescopes. Corning did not use its optical grade glass, and no optical surface finish was specified. The 1723 $AlSiO_3$ tempered windows were of lower quality than the thermal, fused-silica pane. The stresses introduced in the tempering process probably are the reason for this result.

The 5-in. Celestron telescope yielded better results than the 8-in. Meade telescope; however, both were affected by aberrations induced by the windows which were evident as multiple overlapping images and severe astigmatism (see Photographs in Appendices E and F). The Celestron tended to have less variation in quality in a given FOV. A point-by-point summary of the specific results is given in Section 13.

The AAMRL tests conducted concurrently with the Aerospace test found that the window aberrations become apparent for aperture diameters greater than 2 in. At an aperture of 3 in., the resolution of the optics was degraded moderately, but the AAMRL results still found that this aperture yielded the best resolution.

The cutoff point, at which increasing the aperture fails to increase resolving power, still is unclear. Figure 13 shows the resolving power of a diffraction-limited optical system as it varies with aperture diameter in comparison with a simplified aberration function as it varies with aperture. The aberration function assumes a combination of third order aberrations and varies by $D^{2.9}$ power. This is a very general function; specific windows will have their own particular functions.

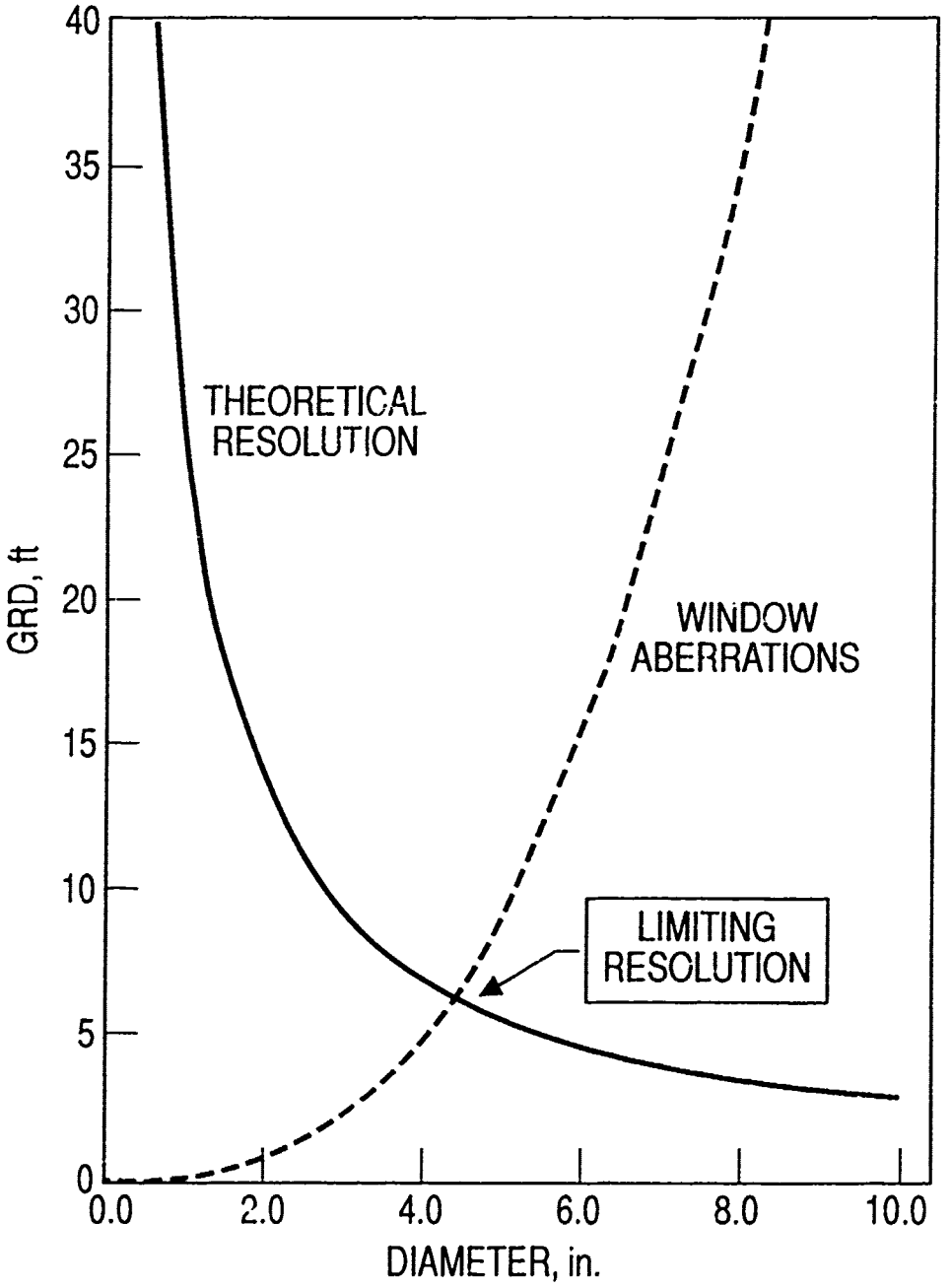

Figure 13. Cutoff Point Between Resolving Power and Aberrations

The intersection of the two functions is the point at which no better resolution will result even by increasing the aperture. For the shuttle windows, this point probably is between 2.5 in. and 3.5 in., depending on the quality of the optical system used.

In conclusion, when an optical system is used in conjunction with a window port, the window must be designed for that use. Space Station Freedom, the Space Shuttle, Spacelab, and Spacehab have the facilities to hold high optical quality windows. For future experiments or programs that require the use of high-resolution optical systems within one of the above facilities, it is critical to design suitable windows to specifically meet these needs.

APPENDIX A:

SPACE SHUTTLE WINDOW LAYOUT

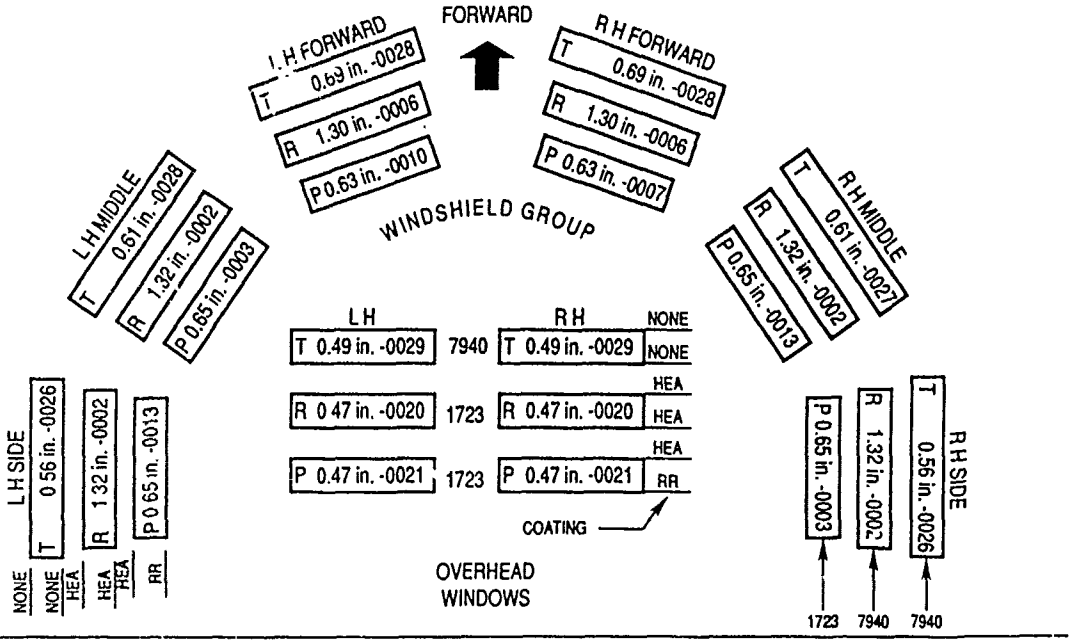

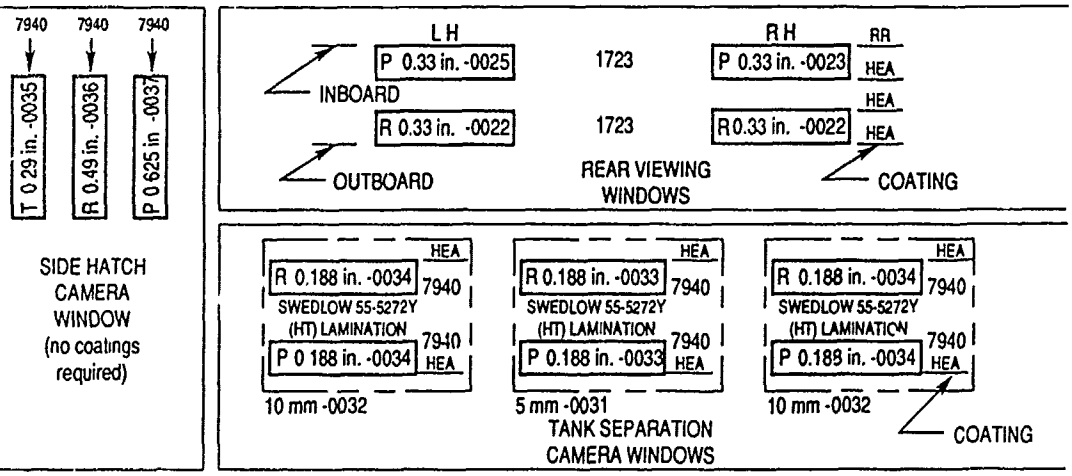

ABOVE PANES, GLASS, THICKNESS, NUMBERS, COATINGS, ET CETERA
PER SPECIFICATION MC332-0006 REV C

WINDOW	QUANTITY REQUIRED	GLASS	LOCATION
-0002	4	7940	WINDSHIELD GROUP LH, RH MID, SIDE
-0003	2	1723	WINDSHIELD GROUP LH MID RH SIDE
-0006	2	7940	WINDSHIELD GROUP LH, RH FORWARD
-0007	1	1723	WINDSHIELD GROUP RH FORWARD
-0010	1	1723	WINDSHIELD GROUP LH FORWARD
-0013	2	1723	WINDSHIELD GROUP LH SIDE RH MID
-0020	2	1723	OVERHEAD GROUP LH RH
-0021	2	1723	OVERHEAD GROUP LH RH
-0022	2	1723	REAR VIEWING GROUP LH, RH OUTBOARD
-0023	1	1723	REAR VIEWING GROUP RH INBOARD
-0025	1	1723	REAR VIEWING GROUP LH INBOARD

WINDOW	QUANTITY REQUIRED	GLASS	LOCATION
-0026	2	7940	WINDSHIELD GROUP LH, RH SIDE
-0027	2	7940	WINDSHIELD GROUP LH RH MIDDLE
-0028	2	7940	WINDSHIELD GROUP UH, RH FORWARD
-0029	2	7940	OVERHEAD GROUP LH, RH
-0031	1	7940	WINDOW ASSEMBLY 5 mm CAMERA
-0032	2	7940	WINDOW ASSEMBLY 10 mm CAMERA
-0033	2	7940	TANK SEP WINDOW 5 mm CAMERA
-0034	4	7940	TANK SEP WINDOW 10 mm CAMERA
-0035	1	7940	SIDE HATCH CAMERA WINDOW
-0036	1	7940	SIDE HATCH CAMERA WINDOW
-0037	1	7940	SIDE HATCH CAMERA WINDOW

APPENDIX B

PHOTOGRAPHS OF HARDWARE AND TEST SETUPS

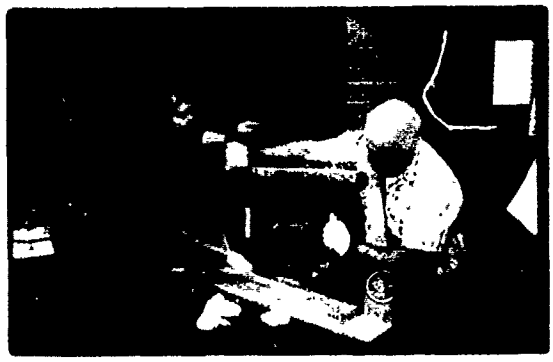

Figure B-1. Window Frame Assembly

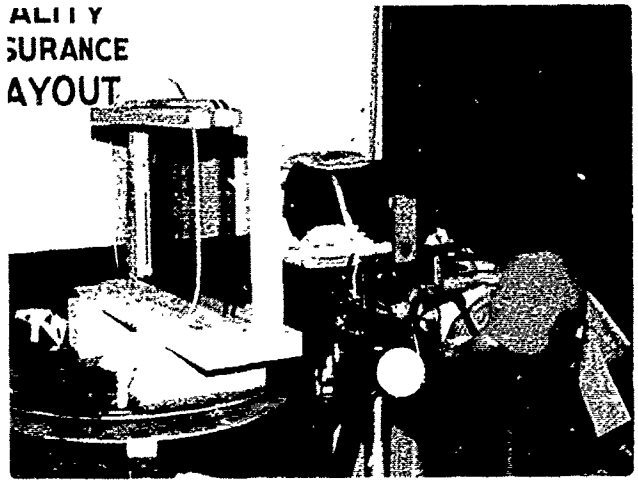

Figure B-2. Window Frame Assembly and Mount

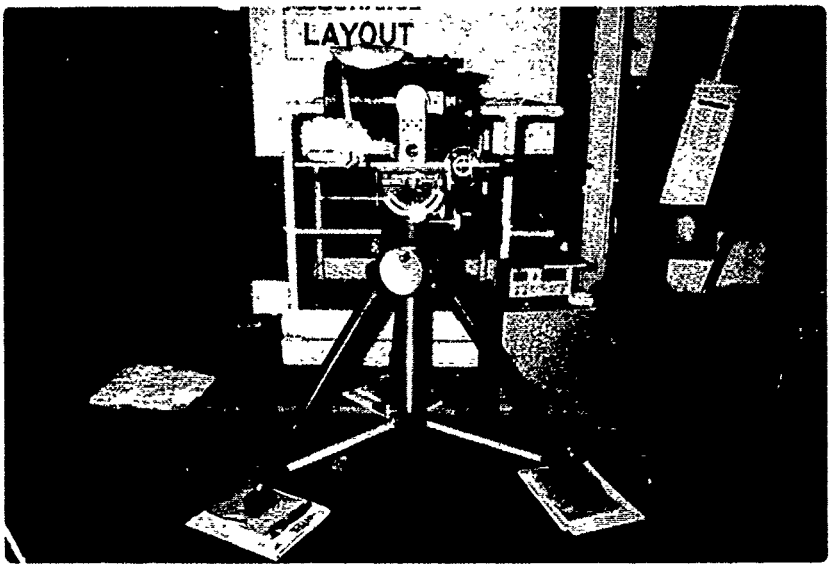

Figure B-3. Meade Assembly

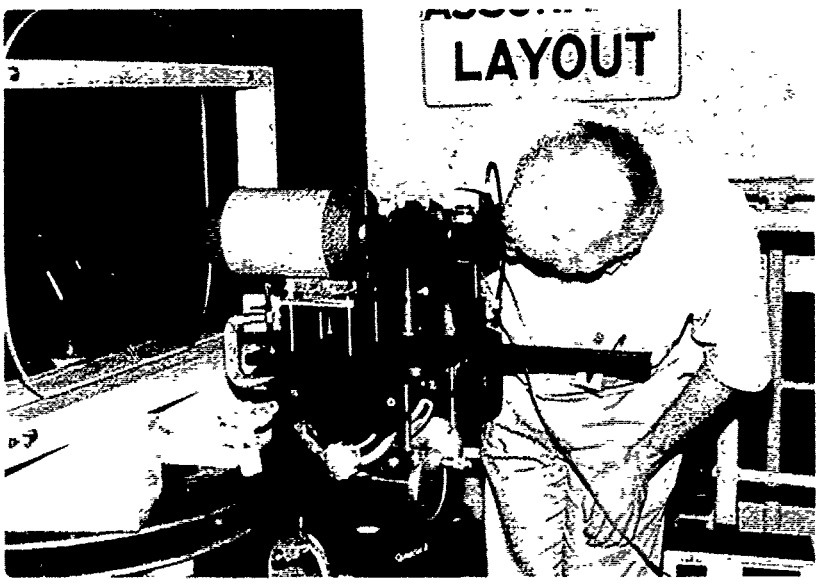

Figure B-4. Celestron Assembly

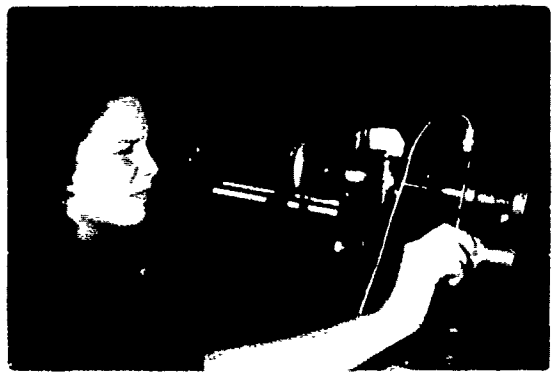

Figure B-5. Photographic Assembly

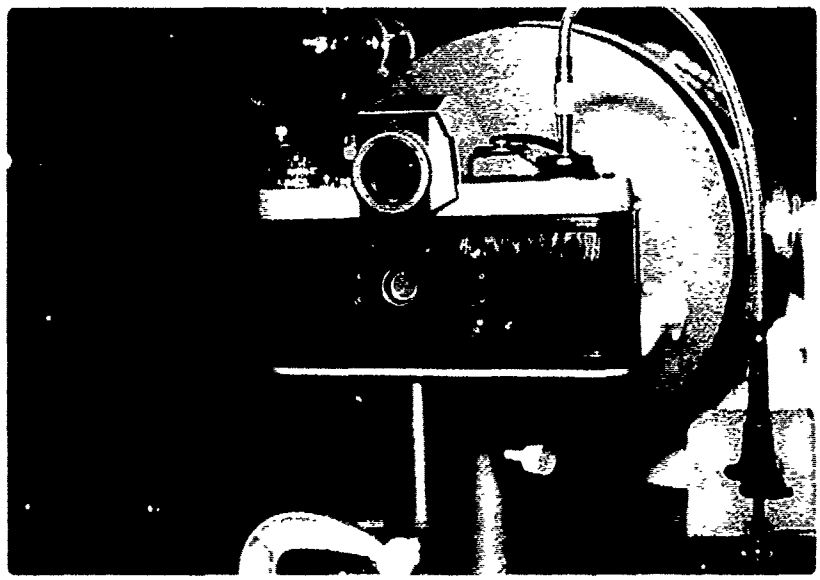

Figure B-6. Removable Modified Camera Back

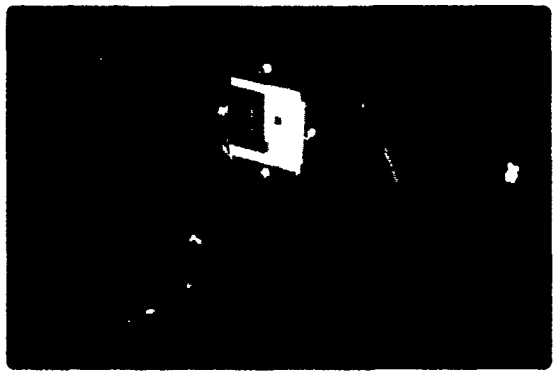

Figure B-7. Tri-Bar Target Assembly

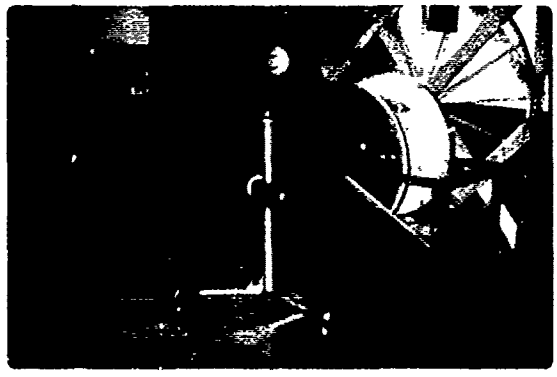

Figure B-8. Tri-Bar Target Assembly on Tripod

Figure B-9. Test Hallway, Tri-Bar Target at Far End

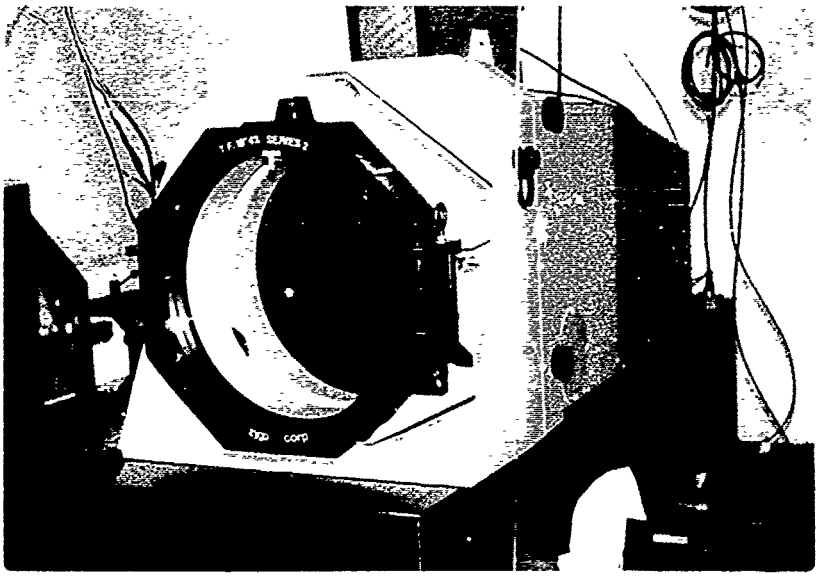

Figure B-10. Zygo Mark IV Interferometer

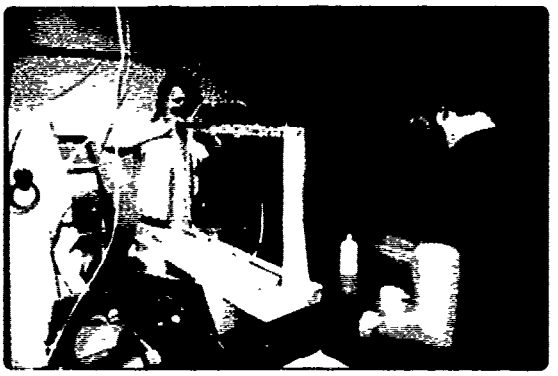

Figure B-11. Zygo with Window Frame

Figure B-12. AAMARL Test with Vivitar Zoo .ens

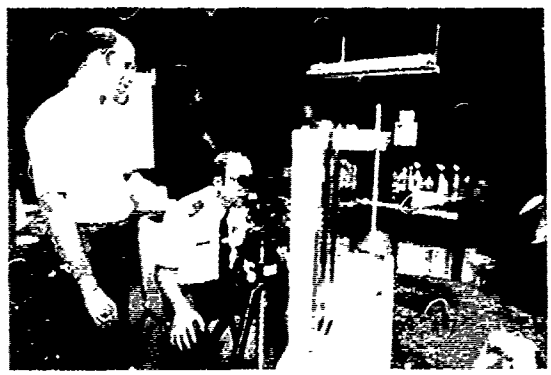

Figure B-13. Vivitar Lens During Window Test at 30°

APPENDIX C

AIR FORCE TRI-BAR TARGET

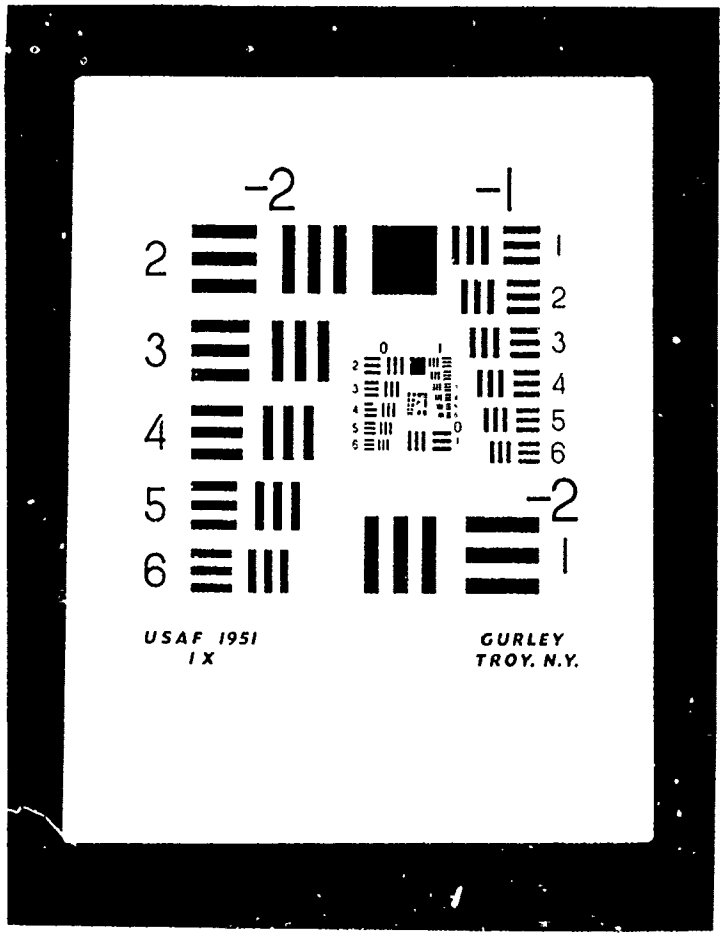
-2
-1
2
3
4
5
6
1
2
3
4
5
6
-2
1
USAF 1951
IX
GURLEY
TROY, N.Y.

APPENDIX D

AIR FORCE DATA SHEETS

PREPARED BY

BUCKBEE MEARS COMPANY

ST. PAUL 1, MINN.

U. S. A. F.
RESOLUTION CHART DATA

NOMENCLATURE AND SPECIFICATIONS

Interval—a line or a space.

Unit—a line and the adjacent space.

Pattern—three lines and two included spaces.

Element—an arrangement of two patterns set at right angles to each other and separated by one unit width.

The proportionality of the line and element dimensions is given by the ratio of the unit widths of two subsequent elements. This ratio shall be the sixth root of two. At the head of every group shall be a group number indicating the number of li/mm of the largest pattern within the group in terms of powers of two. For example, a group number K-3 shall indicate eight li/mm for the largest pattern of this group. The group numbers shall be whole numbers, for example—1, 0, 1 etc. Within a group, every element shall be designated by an element number n=1 (number 1 belonging to the largest element) through number 6 (number 6 belonging to the smallest element). The resolving power R represented by the element n of group K of the target can then be calculated from the equation.

$$R = 2^{K \text{ plus } \frac{n-1}{6}}$$

Thus element 1 of group —2 has 0.25 li/mm, element 1of group —1 has 0.5 li/mm, and element 1 of group 0 has 1 li/mm.

The range of the target shall include ten target groups from 0.25 to 227.5 li/mm or from group —2 to group 7.

GROUP —2

(1) .25 li. m/m	Interval = .07874 Unit = .15748	Element .94488 × .3937
(2) .280625 li. m/m	Interval = .07014699 Unit = .14029398	Element .84176388 × .35073495
(3) .317475 li. m/m	Interval = .06200488225 Unit = .1240097645	Element .744058587 × .31002441125
(4) .356175 li. m/m	Interval = .0552677756 Unit = .1105355513	Element .6632133078 × .27633887825
(5) .3994 li. m/m	Interval = .0492864296 Unit = .0985728592	Element .5914371552 × .246432148
(6) .44545 li. m/m	Interval = .04419126725 Unit = .0883825345	Element .5302952124 × .2209563385

GROUP —1

(1) .50 li. m/m	Interval = .03937 Unit = .07874	Element .47244 × .19685
(2) .56125 li. m/m	Interval = .03507349665 Unit = .07014699	Element .4208819598 × .17536748325
(3) .63495 li. m/m	Interval = .0310024411 Unit = .0620048822	Element .3720292932 × .1550122055
(4) .71235 li. m/m	Interval = .0276338878 Unit = .0552677756	Element .3316066536 × .138169439
(5) .7999 li. m/m	Interval = .0246432148 Unit = .0492864296	Element .2957185776 × .123216074
(6) .8909 li. m/m	Interval = .0220956336 Unit = .0441912672	Element .2651476032 × .110478168

GROUP ÷ 0

(1) 1 li. m/m
Interval = .019685
Unit = .03937
Element .23622 × .098425

(2) 1.1225 li. m/m
Interval = .01753674832
Unit = .03507349665
Element .2104409799 × .087683741625

(3) 1.2599 li. m/m
Interval = .01550122056
Unit = .03100244113
Element .18601464678 × .077506102825

(4) 1.4142 li. m/m
Interval = .01381694391
Unit = .02763388783
Element .16580332698 × .069084719575

(5) 1.5874 li. m/m
Interval = .01232160741
Unit = .02464321482
Element .14785928892 × .06160803705

(6) 1.7818 li. m/m
Interval = .01104781681
Unit = .02209563362
Element .13257380172 × .05523908405

GROUP ÷ 1

(1) 2 li. m/m
Interval = .0098425
Unit = .019685
Element .11811 × .0492125

(2) 2.245 li. m/m
Interval = .00876837416
Unit = .01753674832
Element .10522048992 × .0438418708

(3) 2.5398 li. m/m
Interval = .00775061028
Unit = .01550122056
Element .0900732335 × 0387530514

(4) 2.8494 li. m/m
Interval = .00690847195
Unit = .01381694391
Element .08290166346 × .034542359775

(5) 3.1952 li. m/m
Interval = .0061608037
Unit = .01232160741
Element .07392964446 × .030804018525

(6) 3.5836 li. m/m
Interval = .0055229084
Unit = .01104781681
Element .06628690086 × .027619542025

GROUP ÷ 2

(1) 4 li. m/m
Interval = .00492125
Unit = .0098425
Element .059055 × .02460625

(2) 4.49 li. m/m
Interval = .00438418708
Unit = .00876837416
Element .05261024496 × .0219209354

(3) 5.0796 li. m/m
Interval = .00387530514
Unit = .00775061028
Element .04650366168 × .0193765257

(4) 5.6988 li. m/m
Interval = .003454235975
Unit = .00690847195
Element .0414508257 × .017271177375

(5) 6.3904 li. m/m
Interval = .00308040185
Unit = .0061608037
Element .0369648222 × .01540200925

(6) 7.1272 li. m/m
Interval = .0027619542
Unit = .0055239084
Element .0331434504 × .013809771

GROUP ÷ 3

(1) 8 li. m/m
Interval = .002460625
Unit = .00492125
Element .0295275 × .012303125

(2) 8.98 li. m/m
Interval = .002192093541
Unit = .00438418708
Element .02630512248 × .0109604677

(3) 10.1592 li. m/m
Interval = .001937652571
Unit = .003875305142
Element .023251830852 × .009688262855

(4) 11.3976 li. m/m
Interval = .001727117989
Unit = .003454235979
Element .020725415874 × .0086355899475

(5) 12.7808 li. m/m
Interval = .0015402009[illegible]
Unit = .00308040185[illegible]
Element .018482411112 × .007701004[illegible]

(6) 14.2544 li. m/m
Interval = .0013[illegible]
Unit = .0027[illegible]
Element .016571[illegible]

APPENDIX E

MEADE RESULT PHOTOGRAPHS

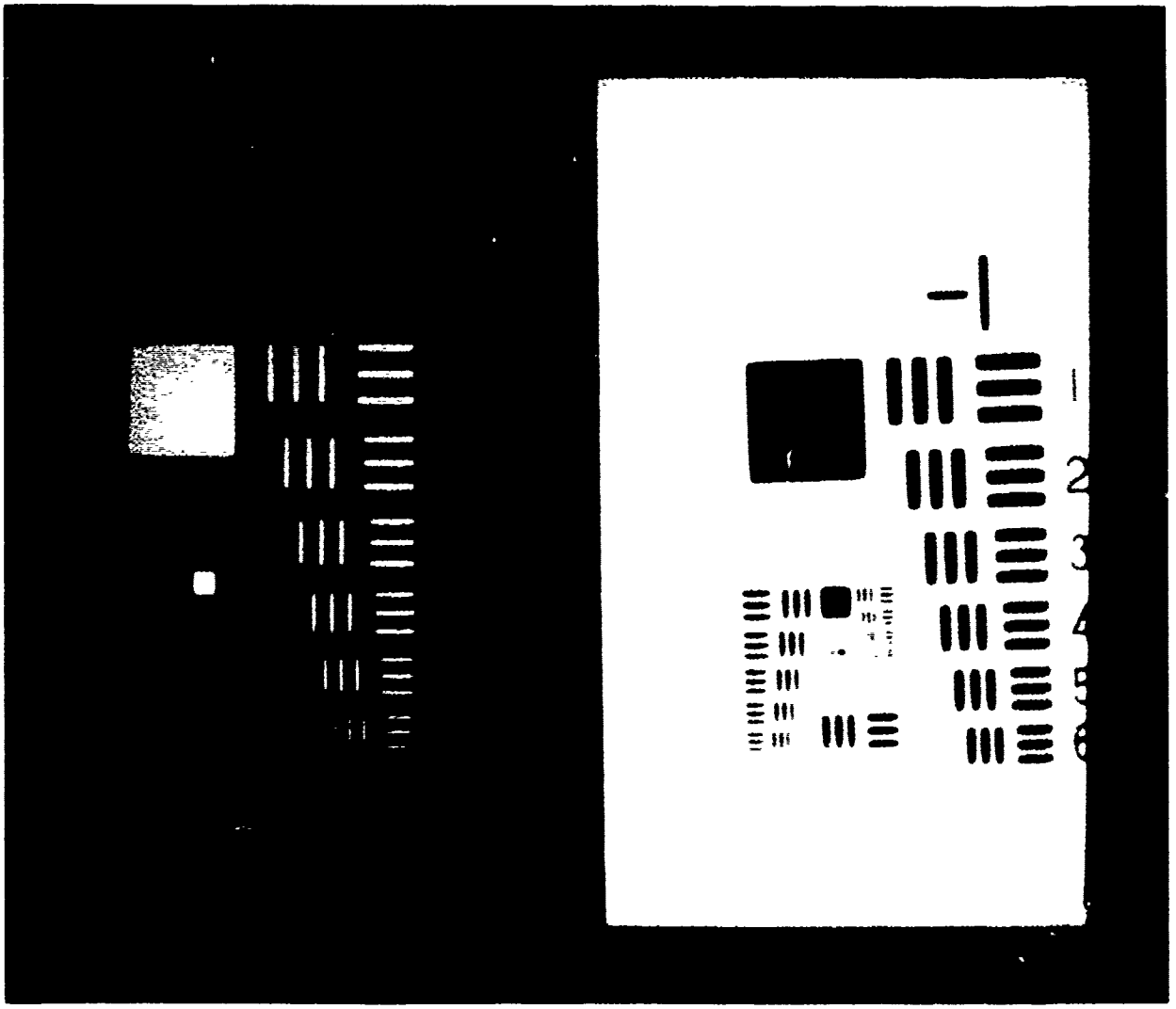

8-inch
Reference
No Windows
10-30a

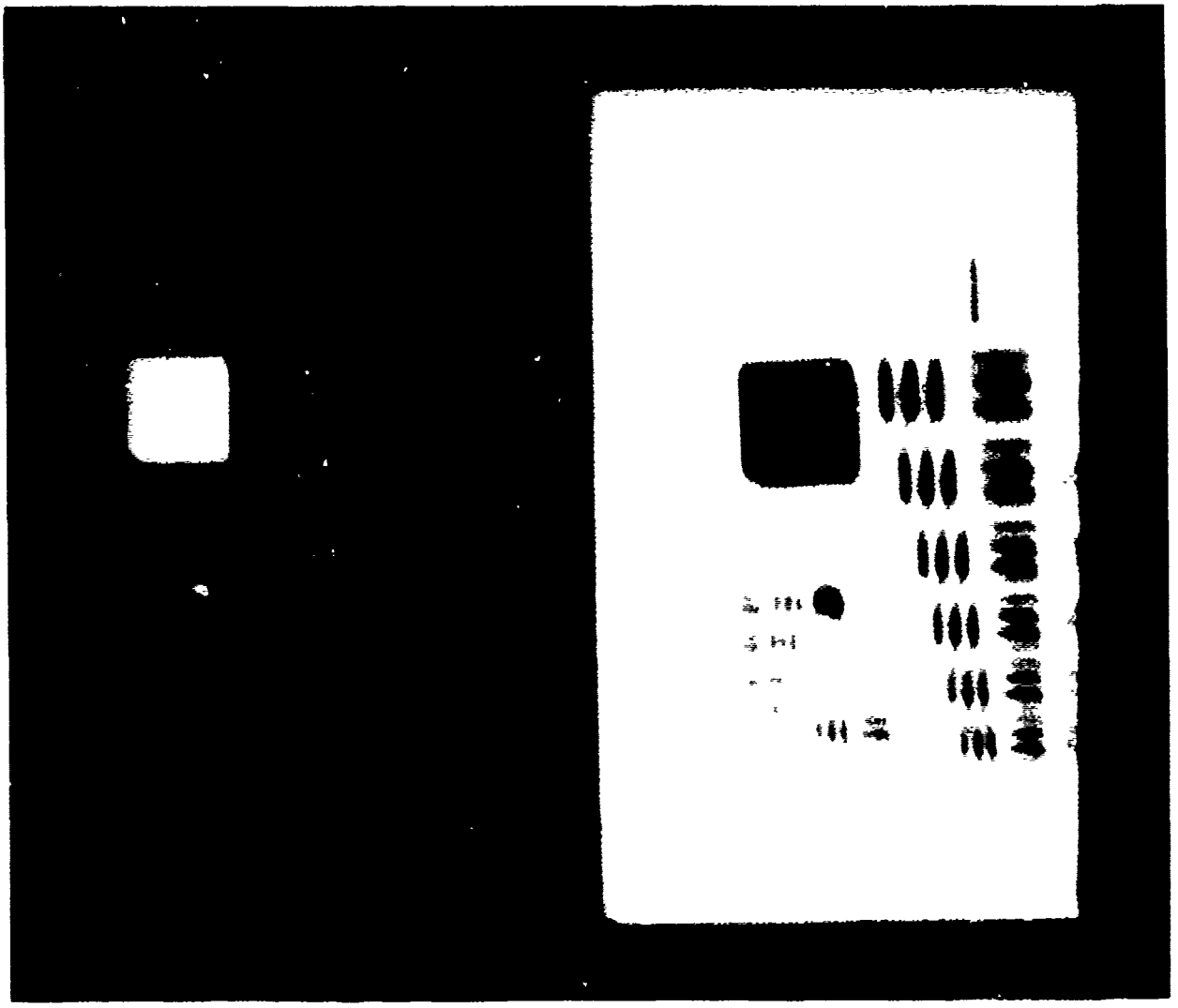

8-inch
Three Panes
Focus Run
11-15a

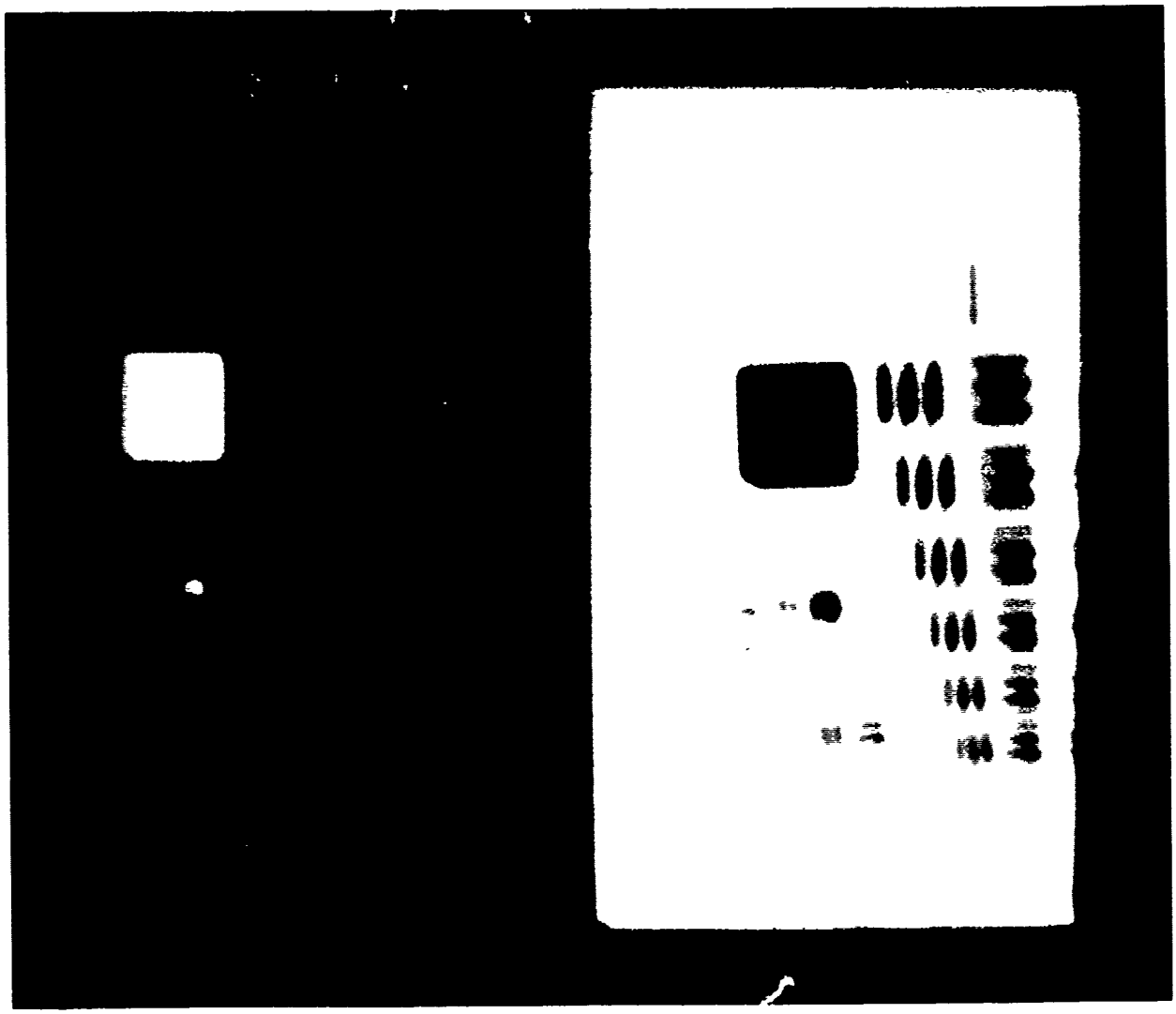

8-inch
Three Panes
Focus Run
11-18a

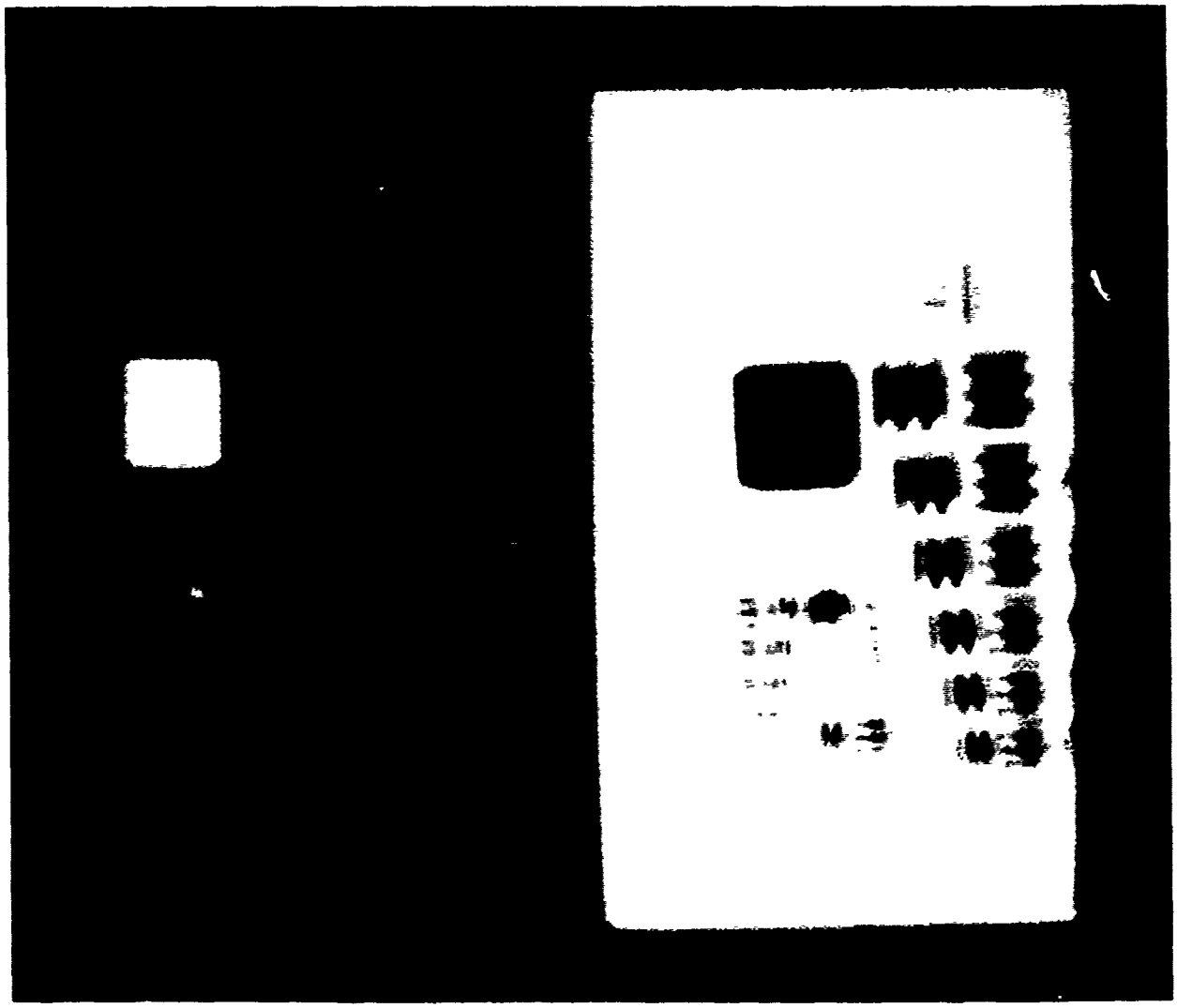

8-inch
Three Panes
Focus Run
11-21a

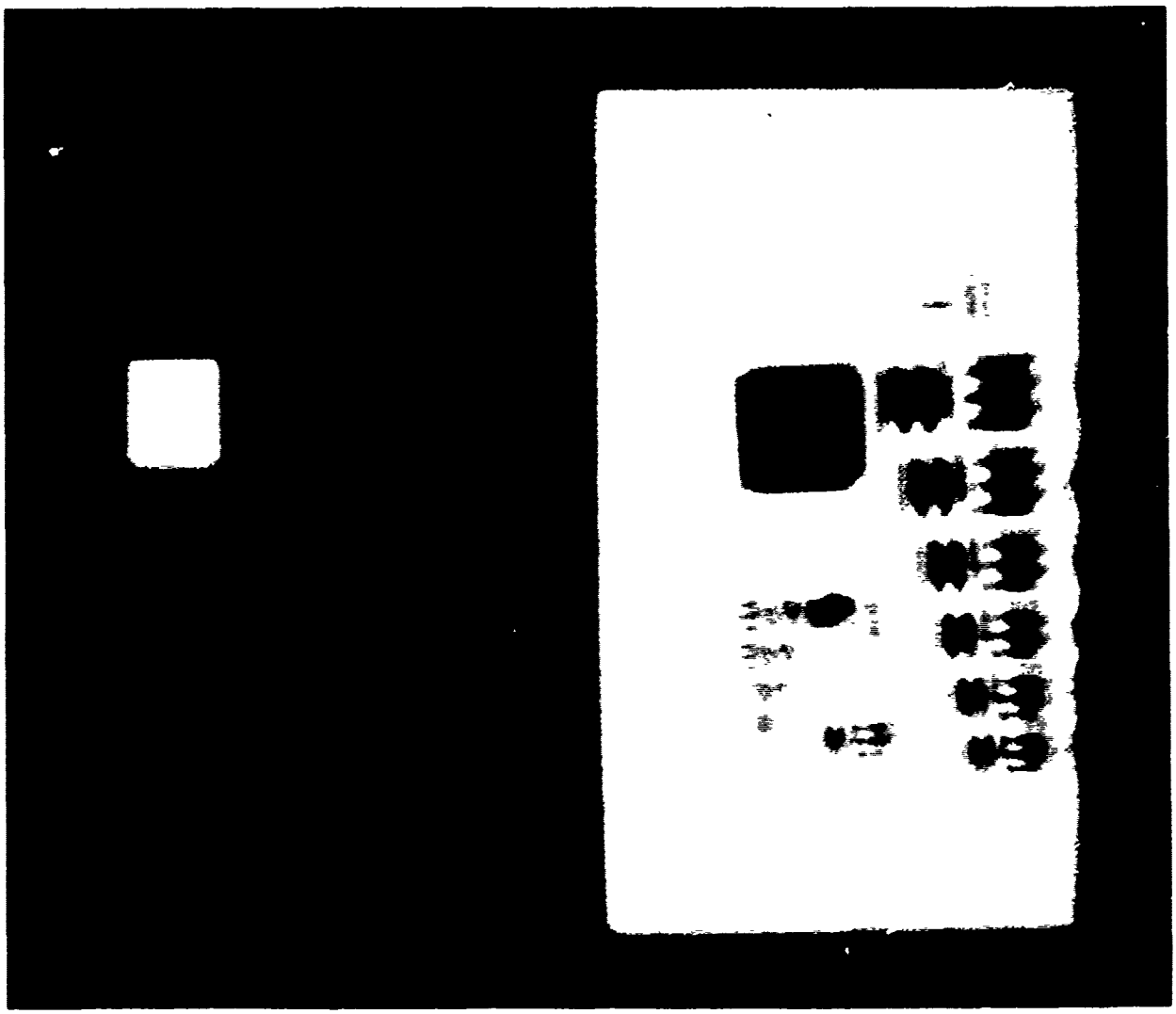

8-inch
Three Panes
Focus Run
11-24a

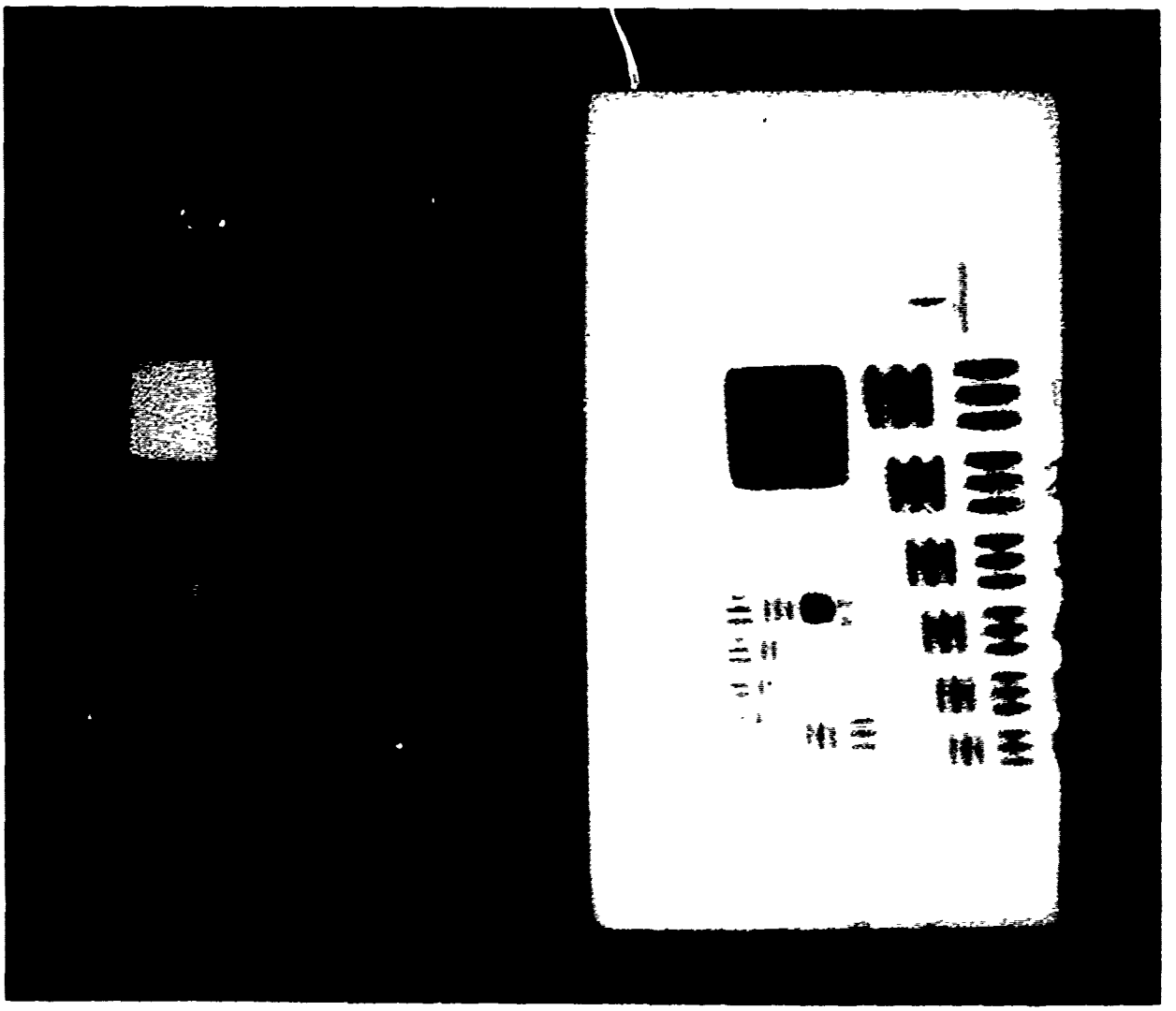

8-inch
Pressure Pane
8-27a

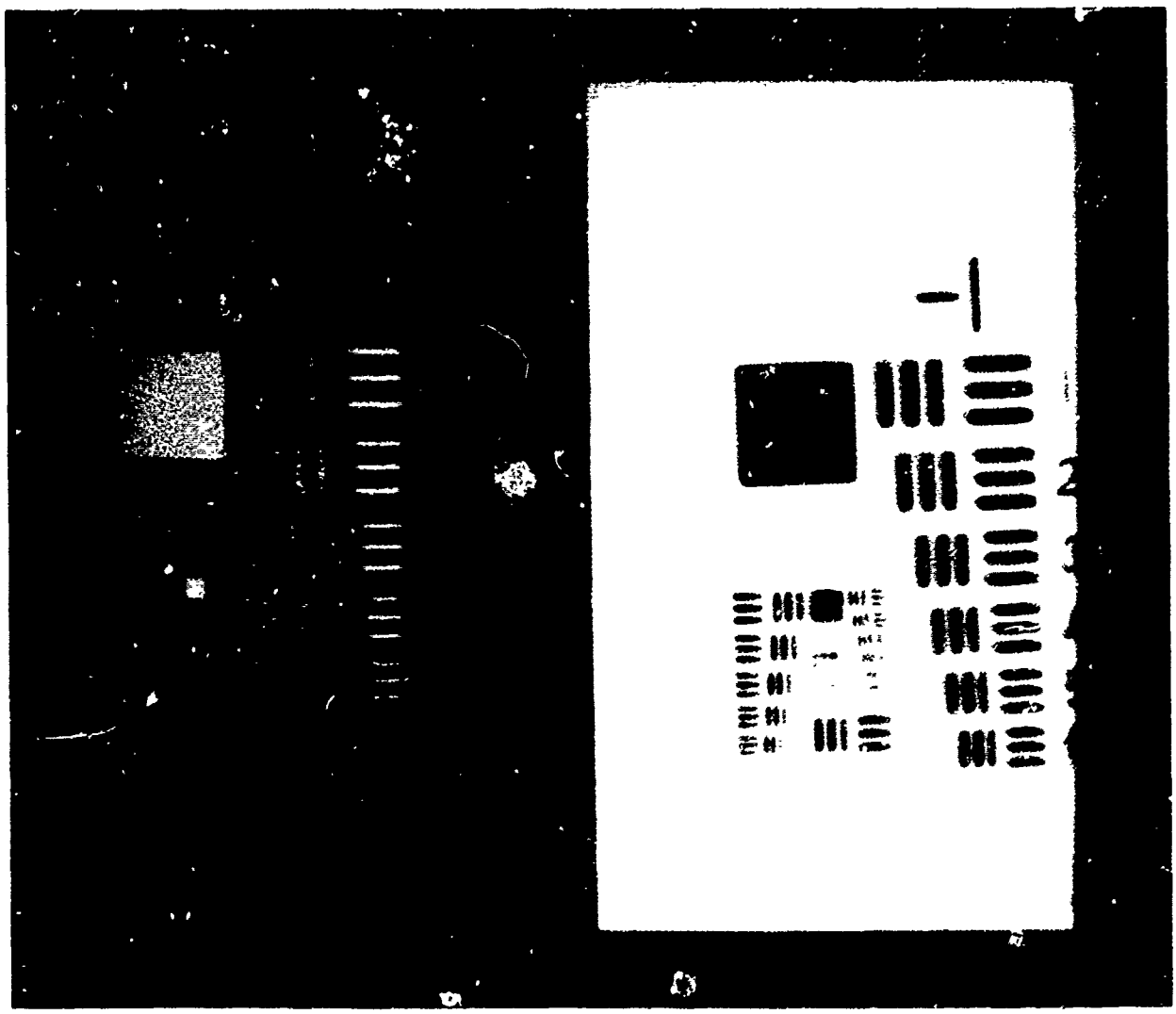

8-inch
Fused Silica
9-28a

APPENDIX F

CELESTRON RESULT PHOTOGRAPHS

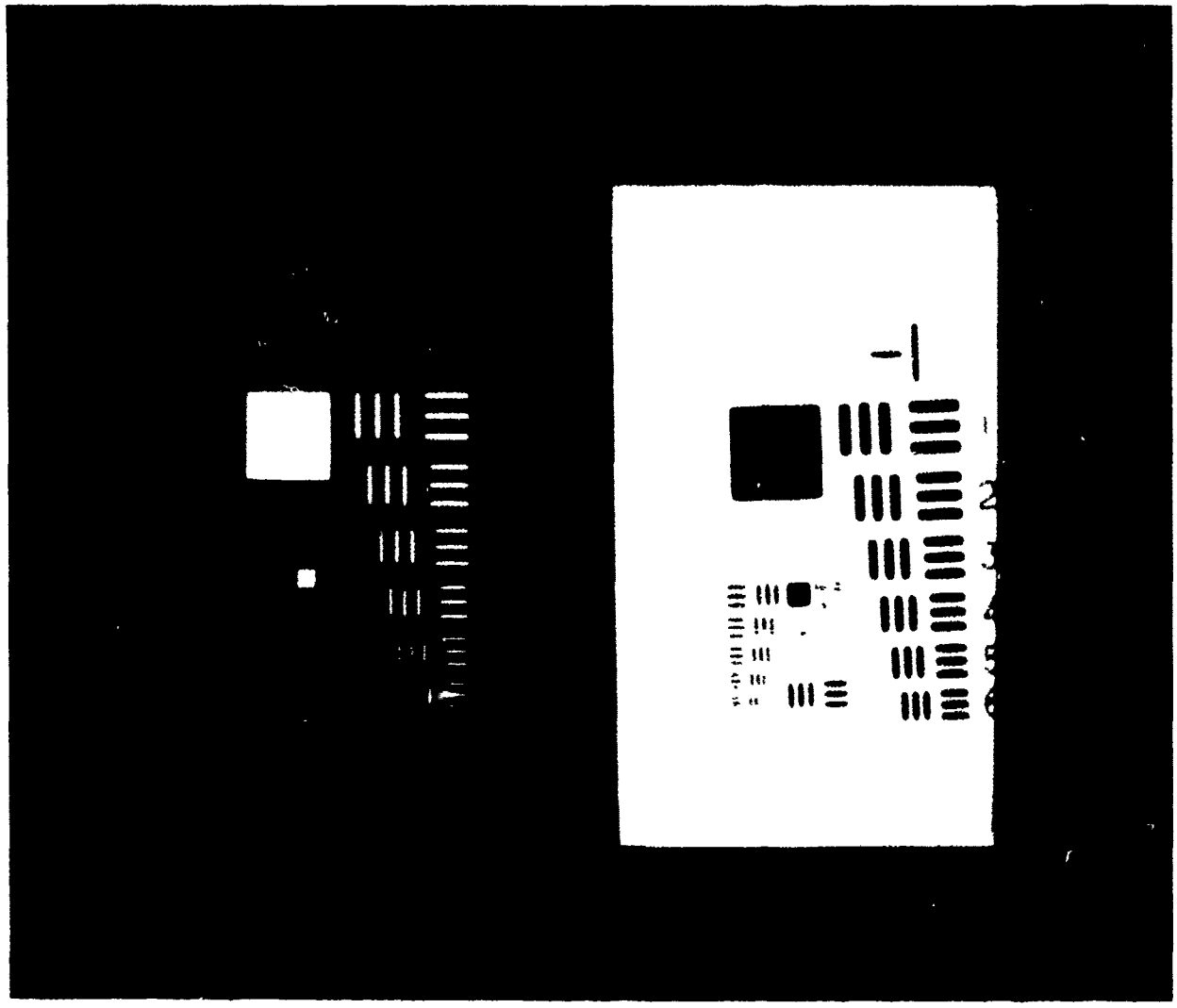

5-inch
Reference
No Windows
13-6a

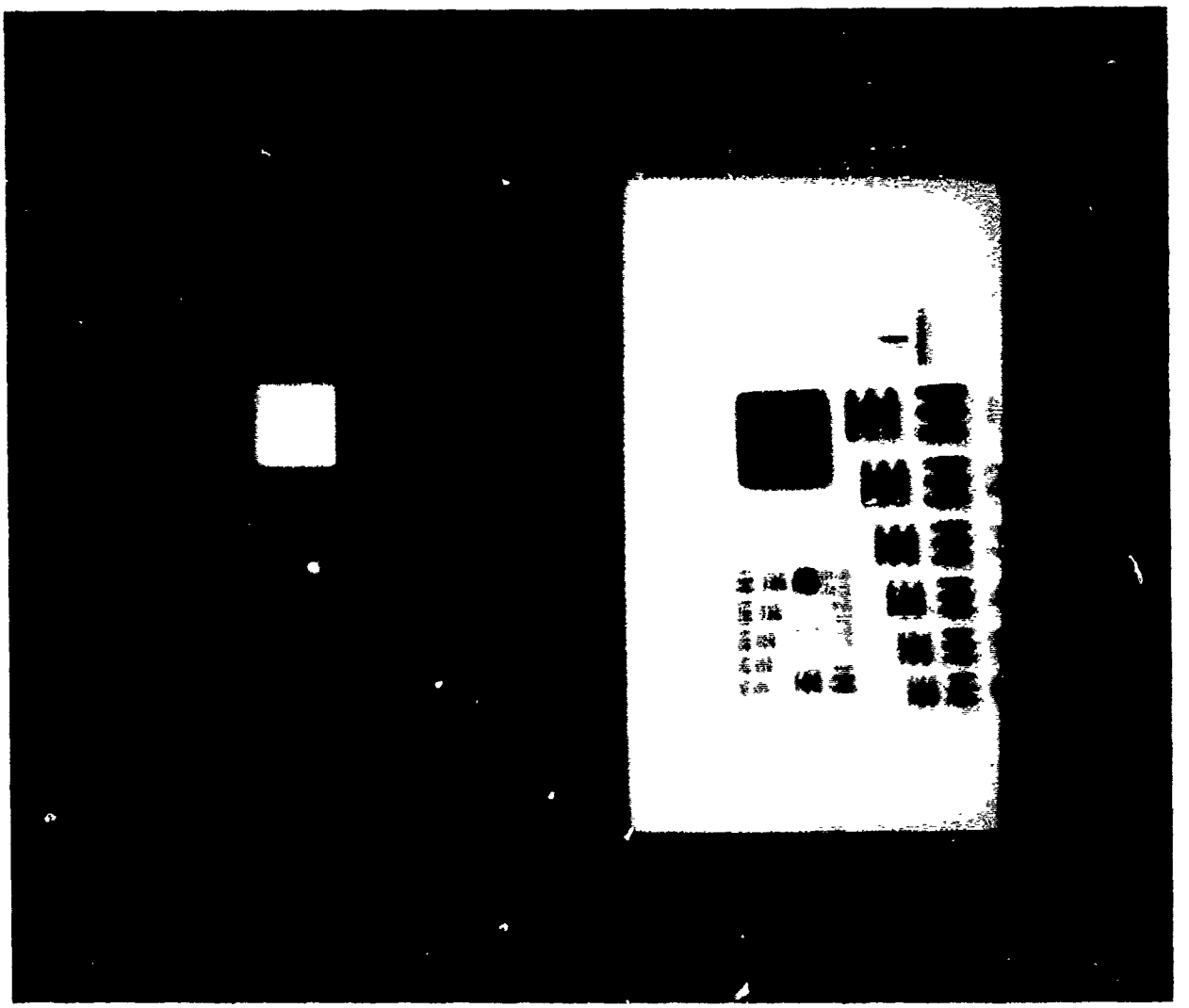

5-inch
Three Panes
12-25a

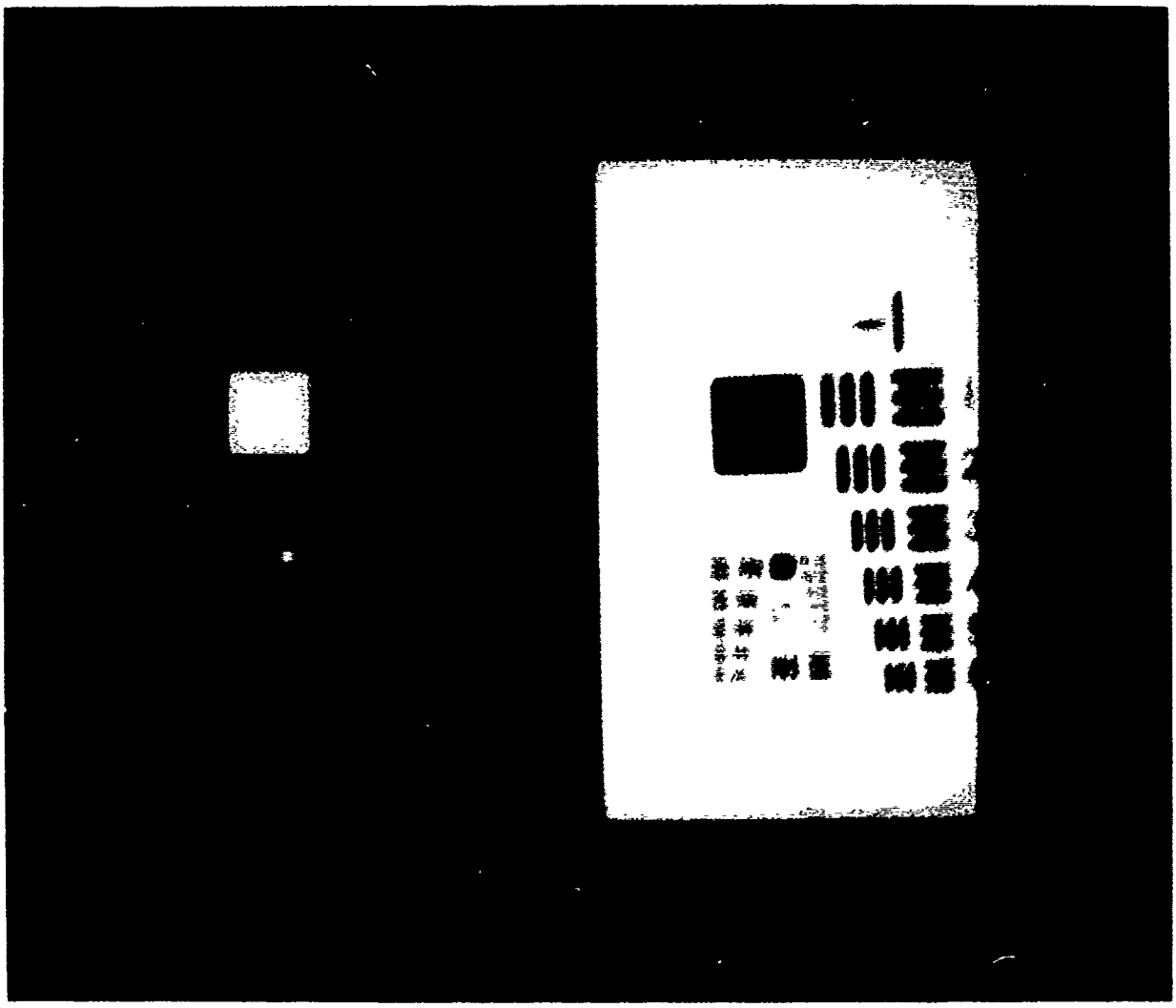

5-inch
Pressure Pane
14-26a

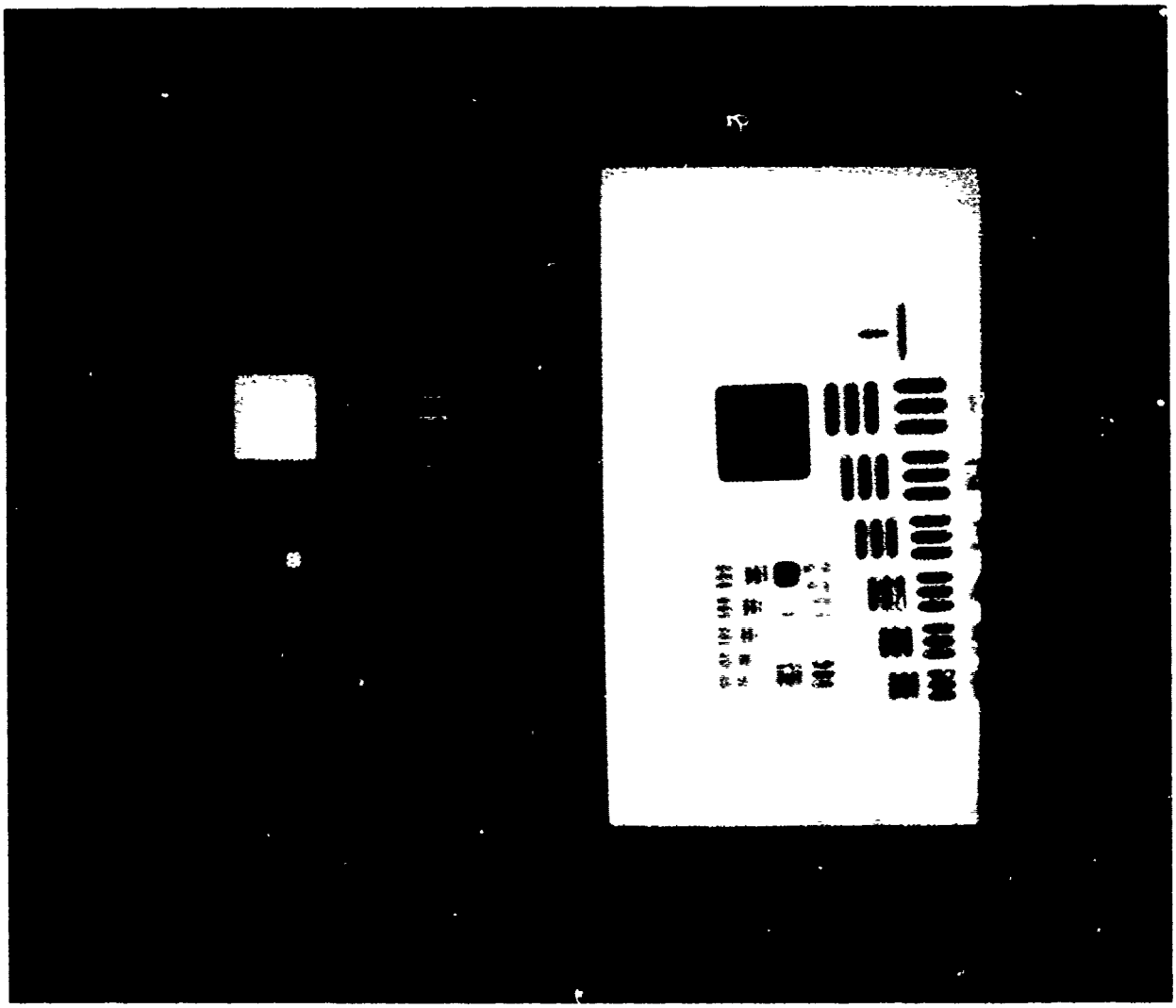

5-inch
Fused Silica
15-9a

APPENDIX G

INTERFEROMETRIC PICTURES

Figure G-1. Center (three panes)

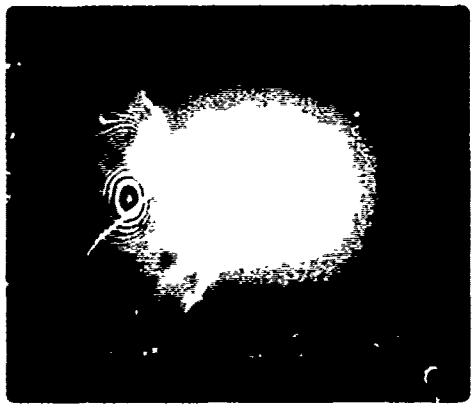

Figure G-2. Upper Right of Three Panes (near tong marks)

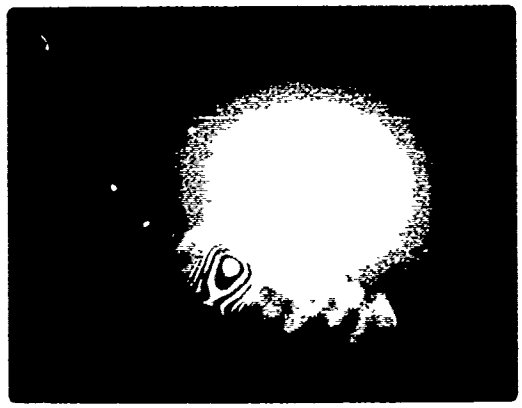

Figure G-3. Lower right (three panes)

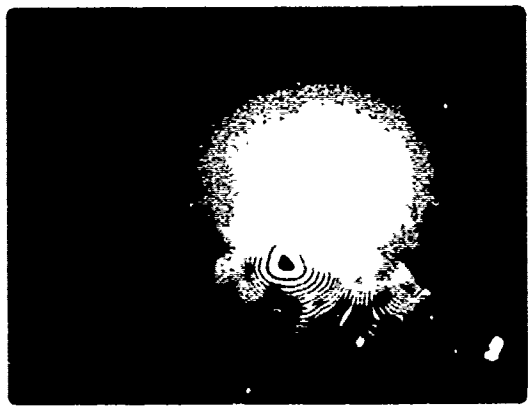

Figure G-4. Bottom Center (three panes)

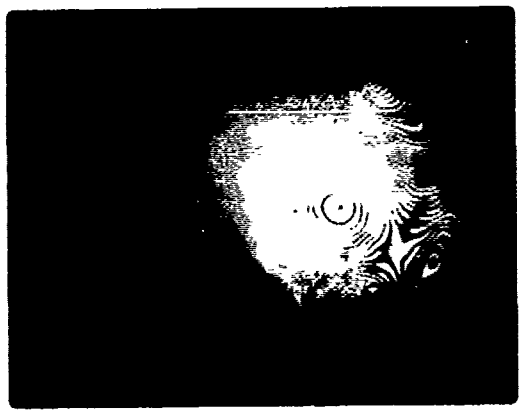

Figure G-5. Lower right (three panes)

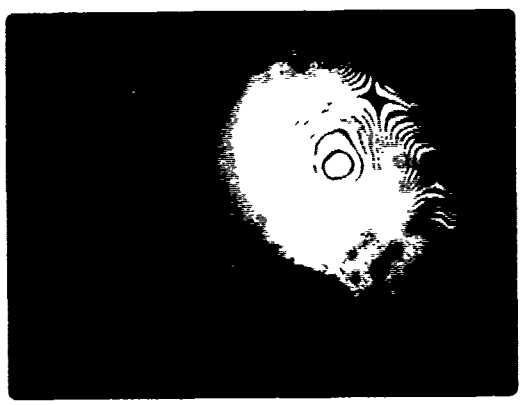

Figure G-6. Upper Right (three panes)

Figure G-7. Center (pressure pane)

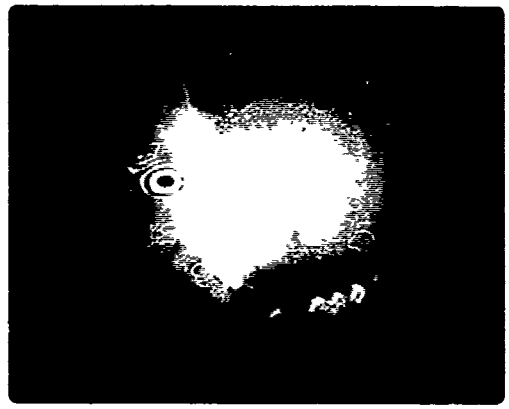

Figure G-8. Upper Left (pressure pane)

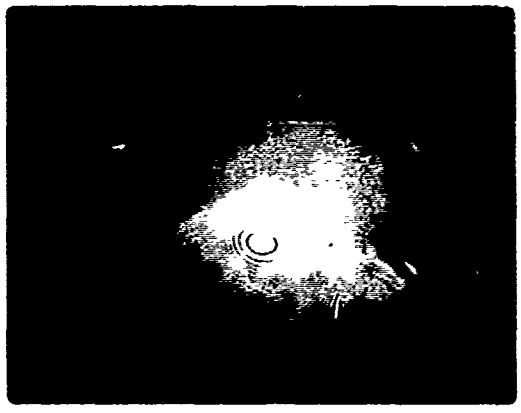

Figure G-9. Lower Center (pressure pane)

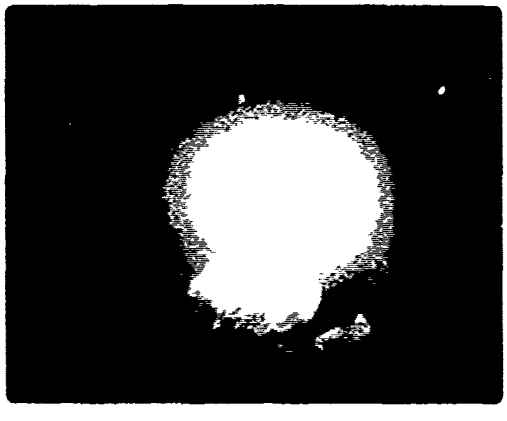

Figure G-10. Bottom (pressure pane)

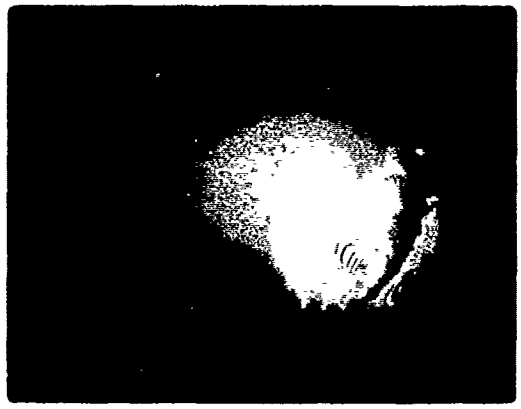

Figure G-11. Lower Right (pressure pane)

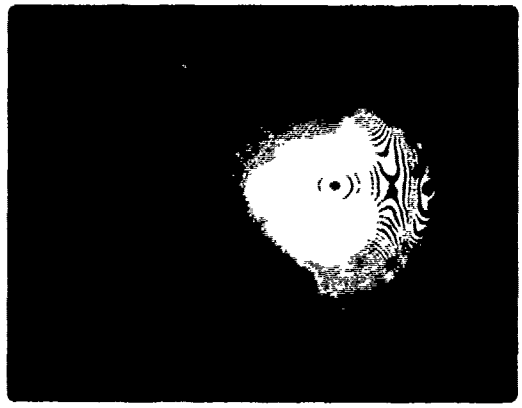

Figure G-12. Upper Right (pressure pane)

Figure G-13. Center (redundant pane)

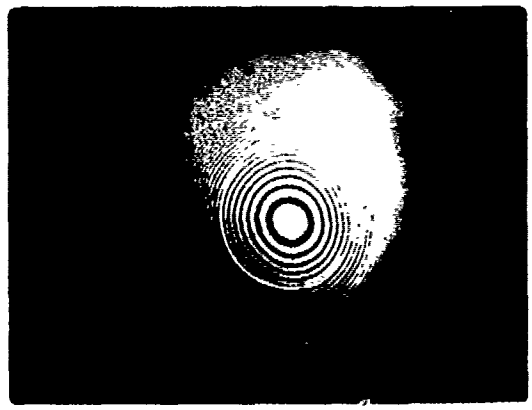

Figure G-14. Center (fused-silica pane)

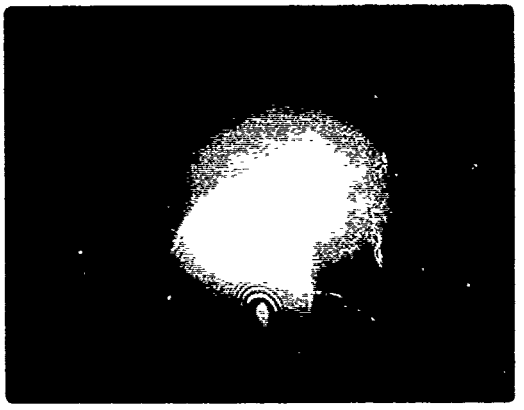

Figure G-15. Bottom (fused silica)

Figure G-16. Top (fused silica)

APPENDIX H

ORIGINAL ZYGO DATA

Three panes in flight configuration
4.5-in. aperture in center

*** WAVEFRONT ***

02-AUG-1989/10:25:37
Part ID :
Serial # :
Analysis : phase
F/NO : plano Fast : off
Averages : 4 Trim : 0
Calibrate: ON AGC : ON
Wave Out : 0.6328 Scale: 0.50
Reference: none
Remove : TLT PWR

PV : 1.160 PTS : 10080
RMS 0.221

	MAGNITUDE	ANGLE
POWER	4.1113	N/A

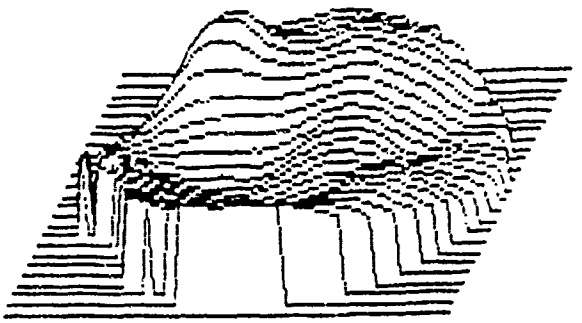

*** ZERNIKE ANALYSIS - 9 terms ***

02-AUG-1989/10:25:37
Part ID :
Serial # :
Analysis : phase
F/NO : plano Fast : off
Averages : 4 Trim : 0
Calibrate: ON AGC : ON
Wave Out : 0.6328 Scale: 0.50
Reference: none
Remove : TLT PWR

--- 3rd ORDER ABERRATIONS ---

	MAGNITUDE	ANGLE
TILT	1.0648	127.23
POWER	4.8079	
ASTIG	0.9299	-89.13
COMA	1.2705	-111.12
SA3	-0.6174	

COEFFICIENTS				
TILT	POWER	4th ORD	6th ORD	TERM
-0.7816	-0.9152	-0.9495	0.0000	1
0.3777	0.2447	0.0577	0.0000	2
	2.0556	0.0953	0.0000	3
		-0.4647	0.0000	4
		-0.0141	0.0000	5
		-0.1526	0.0000	6
		-0.3959	0.0000	7
		-0.1029	0.0000	8
			0.0000	9
			0.0000	10
			0.0000	11
			0.0000	12
			0.0000	13
			0.0000	14
			0.0000	15

RMS	
TILT	0.9990
POWER	0.2211
4th ORDER	0.1053
6th ORDER	0.0030

Redundant pane (0020)

3.5-in. aperture in center

*** WAVEFRONT ***

02-AUG-1989/11:48:57
Part ID :
Serial # :
Analysis : phase
F/NO : plano Fast : off
Averages : 4 Trim : 0
Calibrate: ON AGC : ON
Wave Out : 0.6328 Scale: 0.50
Reference: none
Remove : TLT PWR

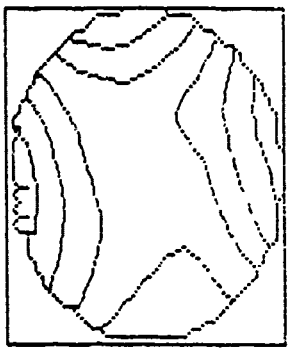

step size 0.36

PV : 1.532 PTS : 8124
RMS : 0.281

	MAGNITUDE	ANGLE
POWER	3.1361	N/A

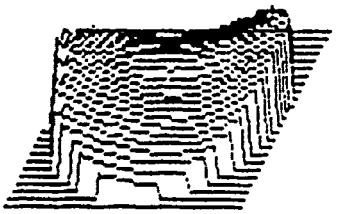

*** ZERNIKE ANALYSIS - 9 terms ***

02-AUG-1989/11:48:57
Part ID :
Serial # :
Analysis : phase
F/NO : plano Fast : off
Averages : 4 Trim : 0
Calibrate: ON AGC : ON
Wave Out : 0.6328 Scale: 0.50
Reference: none
Remove : TLT PWR

--- 3rd ORDER ABERRATIONS ---

	MAGNITUDE	ANGLE
TILT	0.3601	-103.85
POWER	3.7330	
ASTIG	1.6035	10.80
COMA	0.2472	-74.03
SA3	-0.2972	

------- RMS -------

TILT	0.8509
POWER	0.2814
4th ORDER	0.0378
6th ORDER	0.0000

---------- COEFFICIENTS ----------

TILT	POWER	4th ORD	6th ORD	TERM
-0.1032	-0.0585	-0.0409	0.0000	1
-0.4974	-0.5015	-0.5081	0.0000	2
	1.5680	1.7179	0.0000	3
		0.7454	0.0000	4
		0.2952	0.0000	5
		0.0227	0.0000	6
		-0.0792	0.0000	7
		-0.0495	0.0000	8
			0.0000	9
			0.0000	10
			0.0000	11
			0.0000	12
			0.0000	13
			0.0000	14
			0.0000	15

Fused silica

3-in. aperture in center

*** WAVEFRONT ***

02-AUG-1989/12:13:27
Part ID :
Serial # :
Analysis : phase
F/NO : plano Fast : off
Averages : 4 Trim : 0
Calibrate: ON AGC : ON
Wave Out : 0.6328 Scale: 0.50
Reference: none
Remove : TLT PWR

PV : 0.629 PTS : 8172
RMS : 0.117

	MAGNITUDE	ANGLE
POWER	-2.3155	N/A

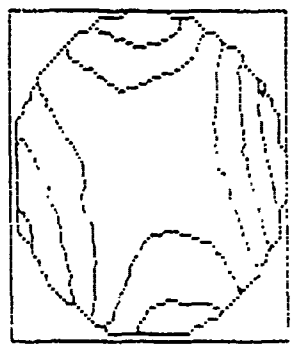

step size 0.10

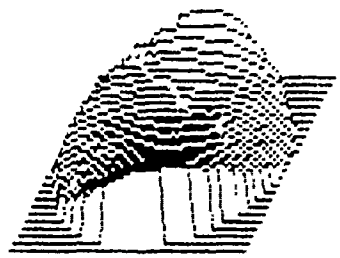

*** ZERNIKE ANALYSIS - 9 terms ***

02-AUG-1989/12:13:27
Part ID :
Serial # :
Analysis : phase
F/NO : plano Fast : off
Averages : 4 Trim : 0
Calibrate: ON AGC : ON
Wave Out : 0.6328 Scale: 0.50
Reference: none
Remove : TLT PWR

--- 3rd ORDER ABERRATIONS ---

	MAGNITUDE	ANGLE
TILT	0.5296	-82.26
POWER	-2.4204	
ASTIG	0.6498	-78.41
COMA	0.0787	109.00
SA3	-0.0235	

	COEFFICIENTS				
	TILT	POWER	4th ORD	5th ORD	TERM
	0.0129	0.0506	0.0543	0.0000	1
	-0.4805	-0.4805	-0.4751	0.0000	2
		-1.1577	-1.2219	0.0000	3
			-0.2987	0.0000	4
			-0.1279	0.0000	5
			-0.0085	0.0000	6
			0.0249	0.0000	7
			-0.0039	0.0000	8
				0.0000	9
				0.0000	10
				0.0000	11
				0.0000	12
				0.0000	13
				0.0000	14
				0.0000	15

RMS	
TILT	0.6041
POWER	0.1130
4th ORDER	0.0221
5th ORDER	0.0000

Pressure pane (0021)

5.5-in. aperture in center

Serial #
Analysis : Phase
F/NO : plano Fast : off
Averages : 4 Trim : 0
Calibrate: ON AGC : ON
Wave Out : 0.6328 Scale: 0.50
Reference: none
Remove : TLT PWR

PV : 2.017 PTS : 10516
RMS : 0.304

	MAGNITUDE	ANGLE
POWER	5.1600	N/A